4-2018

Design and development of a multifunctional surgical device for ground and space-based surgical applications.

Brooke Elaine Barrow
University of Louisville

DESIGN AND DEVELOPMENT OF A MULTIFUNCTIONAL SURGICAL DEVICE
FOR GROUND AND SPACE-BASED SURGICAL APPLICATIONS

By

Brooke Elaine Barrow
B.S., University of Louisville, 2017

A Thesis
Submitted to the Faculty of the
University of Louisville
J.B. Speed School of Engineering
as Partial Fulfillment of the Requirements
for the Professional Degree

MASTER OF ENGINEERING

Department of Bioengineering

April 2018

DESIGN AND DEVELOPMENT OF A MULTIFUNCTIONAL SURGICAL DEVICE
FOR GROUND AND SPACE-BASED SURGICAL APPLICATIONS

Submitted by:
Brooke E. Barrow
B.S., University of Louisville, 2017

A Thesis Approved On

April 26th, 2018

by the following Reading and Examination Committee:

_____
Thomas J. Roussel, PhD, Thesis Director

_____
Ayman El-Baz, PhD, Committee Member

_____
George M. Pantalos, PhD, Committee Member

_____
M. Keith Sharp, ScD, Committee Member

ACKNOWLEDGMENTS

I would like to thank Dr. Thomas Roussel and Dr. George Pantalos for their teaching and mentorship over the past two years. Working on this project has taught me a great deal about scientific research, the design process, and how to "learn by doing". I am grateful for the opportunity to contribute to such an innovative and fascinating research project. I would also like to thank Dr. Keith Sharp and Dr. Ayman El-Baz for their guidance and support throughout this process as members of my thesis committee.

To the UofL Department of Bioengineering, I am appreciative for the opportunity to learn from such brilliant and committed faculty members. My professors have taught me how think critically about science and engineering and I look forward to applying these skills as I pursue a career in medicine.

This project would not be possible without the financial support from the NASA Flight Opportunities Program (Grant NNX16AC59G). I would also like to thank the UofL National Science Foundation (NSF) Innovation Corps (I-Corps) Program for providing monetary support for prototype development.

Finally, I would like to thank my family. To my brother James, thank you for sharing your interest in science with me. I am excited to watch you grow as you soon transition to college. To my parents, thank you for the continuous love and encouragement as I pursue my education. I truly could not ask for better role models and supporters.

ABSTRACT
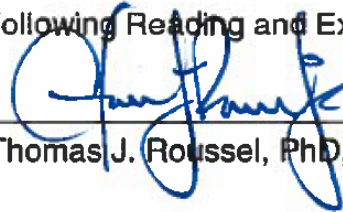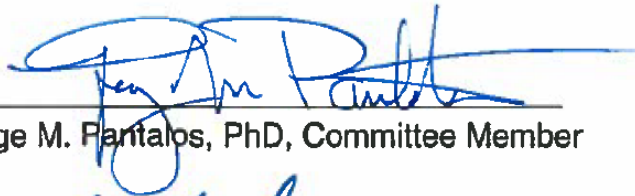
DESIGN AND DEVELOPMENT OF A MULTIFUNCTIONAL SURGICAL DEVICE
FOR GROUND AND SPACE-BASED SURGICAL APPLICATIONS

Brooke E. Barrow

With the possibility of longer ventures into space, NASA will face many
new medical challenges. The ability to surgically treat trauma and other disorders
in reduced gravity requires reliable wound access, containment, and
visualization. In collaboration with Carnegie Mellon University, the University of
Louisville is currently developing the AISS (Aqueous Immersion Surgical System)
to increase efficiency and control of the operative field in space-based surgeries.
Reliable wound access and containment is achieved by placing a transparent
wound-isolation dome securely over the wound-site and pressurizing it with a
saline solution. Leak-free trocars provide access ports for various surgical
instruments. This system will prevent contamination of the environment from
blood and other bodily fluids, control bleeding, provide a sterile microenvironment
for surgical intervention, and maintain visualization of the operative field.

The objective of this project is to develop a Multifunctional Surgical Device
(MFSD) that is compatible will the AISS system and conventional ground-based
surgical techniques. Economy and efficiency of instrument exchange are

necessary given the limited resources and number of crew members on an exploration space flight. The MFSD aims to provide suction, irrigation, illumination, visualization, and cautery functionality through a single-instrument via finger-tip control. This multifunctionality will reduce intraoperative blood loss and help maintain visualization of the operative field by removing blood and debris. Also, the MFSD will help preserve surgical focus and minimize surgeon manual movement and instrument exchanges. Applicability of the MFSD for ground-based surgical procedures is also anticipated.

This project has been successful in developing a multifunctional device that integrates suction, irrigation, and illumination. Testing of these three functions has been performed on the benchtop and in a live-animal model using a stand-alone control system. After completing the myRIO integration of the MFSD with the Fluid Management System (FMS), further testing will allow for validation of device functionality and efficacy with the AISS. Future work for this project will include preparing for a suborbital space flight of the AISS on the Virgin Galactic SpaceShipTwo planned for later 2018. This flight test will evaluate irrigating, illuminating, and suctioning analog blood from a simulated wound-site in microgravity. The addition of cutting and coagulation cautery and visualization functions is planned for subsequent months. Earth-based development and utilization of the MFSD for surgical procedures is also anticipated.

TABLE OF CONTENTS

LIST OF TABLES

LIST OF FIGURES

I. INTRODUCTION

1.1 Clinical Problem

In 2017, Congress passed the *NASA Transition Authorization Act (TAA) of 2017* to support the Trump Administration's commitment to maintaining the United States' involvement in space and aeronautical research. Further, NASA plans to establish a permanent refueling station on the moon, sponsor a manned mission to an asteroid by 2025, and travel to Mars by the end of the 2030s [1-3]. As NASA anticipates future missions to regions beyond low Earth orbit, the duration of space travel will increase [4]. Among the many problems associated with extended space travel is the ability to administer healthcare to crew members effectively and efficiently since quick return to Earth will not be an option.

In effort to address this challenge, NASA published a Human Health and Life Support Roadmap that outlines the need for a sterile, closed-loop fluid management system [5]. This system will permit the treatment of traumas and other surgically-treatable injuries that have the potential to occur during long-distance space exploration. This technology is critical, as medical evacuation to receive Earth-bound care will not be an option for crew members on these extended journeys (astronauts stationed on the International Space Station can be shuttled down to Earth should a medical situation arise). For this reason, it is

imperative that crew members have sufficient training and are adequately equipped for in-flight medical care. This is especially true considering the complications of performing surgical procedures in what effectively will be zero gravity [4].

The University of Louisville and Carnegie Mellon University have responded to NASA's call for the development of emergency surgical capabilities. Researchers at both institutions are working to develop an Aqueous Immersion Surgical System (AISS). This closed-loop fluid management system can pressurize a translucent chamber to help control bleeding, cleanse the wound via saline irrigation, and maintain a clear visual field during surgical treatment. Electronic feedback mechanisms control the volume and pressure of the fluid system, while instrument feedthroughs in the wall of the chamber allow the medical provider to perform necessary procedures.

Economy and efficiency of instrument exchange will be critical assuming limited resources and a minimal number of crew members on an exploration space flight. Because material resources in space are restricted, a multifunctional surgical device designed to simplify and streamline the surgical procedure presents a significant advantage to flight/medical crew members who may need to perform an emergency procedure (e.g. appendectomy, cholecystectomy). A surgical device with multiple integrated functions will reduce the number of instruments on-board an exploration campaign and reduce the number of instrument exchanges during a surgical procedure.

1.2 Project Goals

The objective of this project is to develop a Multifunctional Surgical Device (MFSD) that integrates suction, irrigation, illumination, visualization, and simultaneous cut and coagulation cautery via finger-tip control in a single instrument. This multifunctionality will ultimately improve and maintain visualization by removing blood and debris, illuminate the operative field, and enhance visualization at the surgical site of interest. A stand-alone control system will permit verification of device functionality in preparation for future integration with the Aqueous Immersion Surgical System (AISS) Fluid Management System that is also currently in development at the University of Louisville. The final integrated system aims to provide the ability to perform surgical procedures in a sterile and closed-loop environment.

Specific Aim 1: Design a multifunctional surgical device that includes suction, irrigation, illumination, and simulated cautery functionality. A clamshell housing assembly should incorporate fluidic pathways for suction and irrigation, a fiber optic for illumination, and pushbuttons for activation of each function. The device design should permit comfortable index-finger device activation.

Specific Aim 2: Develop a fluid system that supports single-channel suction and irrigation at a flow rate appropriate for endoscopic surgical procedures. The system should be occlusive and maintain pressure within the fluid line. In

addition, the system should connect to both an irrigation fluid (e.g. saline) reservoir and waste container.

Specific Aim 3: Develop a stand-alone electronic control system for suction, irrigation, illumination, and simulated cautery. A microcontroller and custom-printed circuit board (PCB) interface should power this system and allow for momentary activation of each function. This will permit device verification in preparation for integration with the AISS system and future testing on a suborbital space flight.

II. BACKGROUND

2.1 Future of Space Exploration

NASA was founded by President Eisenhower in 1958. Since its establishment, the program has pioneered the United States' commitment to scientific discovery, aeronautics research, and space exploration [6]. Neil Armstrong was the first man to walk on the moon in 1969. In 2000, NASA occupied the International Space Station (ISS) [7].

NASA plans to expand its space exploration program for future missions. In 2004, NASA launched the "Vision for Space Exploration" program that projects future missions to the Earth's moon and Mars [7]. Recently, Congress passed the *NASA Transition Authorization Act (TAA) of 2017.* This legislation affirms the Trump Administration and NASA's commitment to space exploration and scientific discovery. Some predict that by the third or fourth decade of the 21st century, there will be outposts on both Earth's moon and Mars [8].

2.2 Medical Considerations

Providing healthcare in space is a unique field of medicine. There are several medical concerns regarding long-duration space missions: extended communication delays with Earth, limited medical supplies, atypical physiological changes, limited/incomplete/inadequate training and experience, radiation

exposure (that may cause some of the strange physiological conditions), and difficulty performing operations in an enclosed environment and in zero gravity [7]. Considering these complications, as space missions increase in duration, medical care for the crewmembers will certainly become more complex [4, 9].

NASA collected data from 89 missions between 1981 and 1998 that indicate several dozen medical events during flight. These events affected nearly all organs and, in some cases, presented a high risk of harm [10]. For instance, in 1982, a Russian astronaut was evacuated from the Salyut 7 Space Station and returned to Earth after developing kidney stones [11]. Fortunately, for individuals stationed on the ISS, the Assured Crew Return Vehicle [12, 13] is available and equipped to return patients in need of medical care to Earth in roughly six (6) to twenty-four (24) hours [14]. For missions to Earth's moon and Mars, this time will increase to several days and months, respectively [15].

In an effort to mitigate risks and maximize mission success, medical standards have been established for space flight participants to ensure they are of good health and capable of executing mission operations [13]. Five flight surgeons determine if an individual is fit for space exploration based on personal and family medical history, lifestyle habits, medications, and numerous lab test results [13, 16].

Telemedicine is also a key component of medical care on the ISS. This involves the direction of a relatively inexperienced medical provider by a remotely placed flight surgeon [12] for consultative, diagnostic, and treatment services [10, 12, 17]. Because this system may require near-instantaneous communication

between the two parties, telemedicine is not likely a feasible option for long-duration space flight due to communication lags. For instance, communication to planet Mars can take 6.5 – 44 minutes [10]. Thus, the presence of an experienced medical professional is critical for long-duration flights.

Several operations have been performed in low-gravity environments (i.e. parabolic and suborbital flights). The first surgical experiment was a laparotomy on a rabbit by Russian scientists in 1967 [10]. In 2006, a team of French surgeons removed a benign tumor from the forearm of a 46-year-old volunteer [18]. When performing a surgical procedure in a low-gravity environment, it is important to consider the physiological changes resulting from a lack of gravity and constant radiation [8]. Many of the effects of microgravity on various medical conditions are still unknown [16].

2.3 Surgical Needs in Space

As spaceflight missions become more frequent and last longer, there is a need for more comprehensive in-flight medical care [12]. Despite health screenings that aim to select the most viable astronauts, life-threatening conditions that necessitate surgical intervention are still possible. Common conditions include appendicitis, intestinal blockage, and cholecystitis [1]. NASA agrees that the most significant threat, however, is trauma [19]. Per the NASA Roadmap for Technology Area document (TA) section "Technology 6.3.2, Long Duration Health":

"Trauma is the most highly prevalent medical issue in long-duration flight, and the ability to perform life-saving surgery after major trauma and other

7

unpredictable life-threatening conditions (e.g., appendicitis) will be very important for exploration class mission to improve crew survivability."

Several studies have demonstrated the feasibility of performing surgical tasks and procedures in microgravity [1, 4, 12, 20, 21]. Some indicate that tasks are no more difficult that in a 1-g environment given proper restraint of the patient, operator, and surgical hardware [12]. Despite this, common concerns about space-surgery include impaired visualization of the surgical area from the absence of gravitational retraction of bowel and/or thoracic organs and visual obstruction from floating blood, tissue debris, and irrigation fluid [12]. Due to extremely long separation from medical care, medical care on long-duration missions should be autonomous and self-sufficient [7]. Further, the surgical hardware must be simple, reliable, and small [12].

2.4 Current Developments

2.4.1 Aqueous Immersion Surgical System

Through funding from the NASA Flight Opportunities Program, the University of Louisville and Carnegie Mellon University have been working simultaneously to develop surgical technologies for space. Specifically, the University of Louisville is developing an Aqueous Immersion Surgical System (AISS), which includes a clear, rigid chamber that is attached to the skin over a wound site, as shown in Figure 1 [22] and Figure 2. The chamber is filled and pressurized with fluid (e.g. saline) to help control bleeding, cleanse the wound, and maintain a clear visual field during surgical treatment. Various transducers and feedback mechanisms control the volume and pressure of the fluid system.
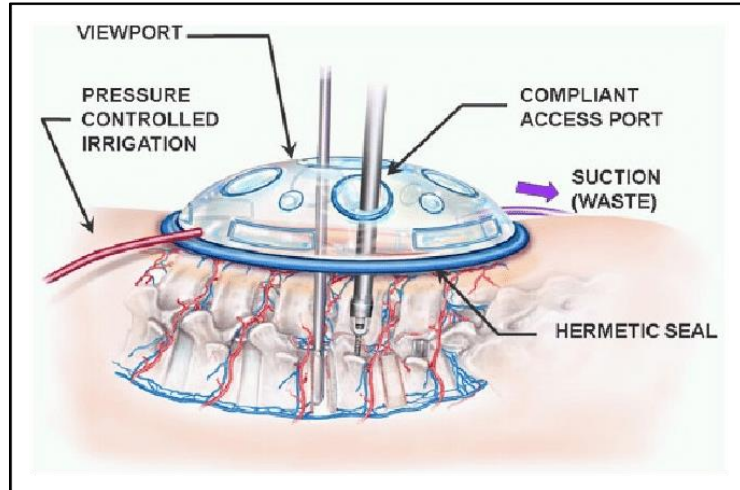
Figure 1 - An artist's rendition of a surgical containment system [22]

Finally, the surgeon can perform necessary procedures via trocars that maintain

pressure and are designed to have minimal leakage.
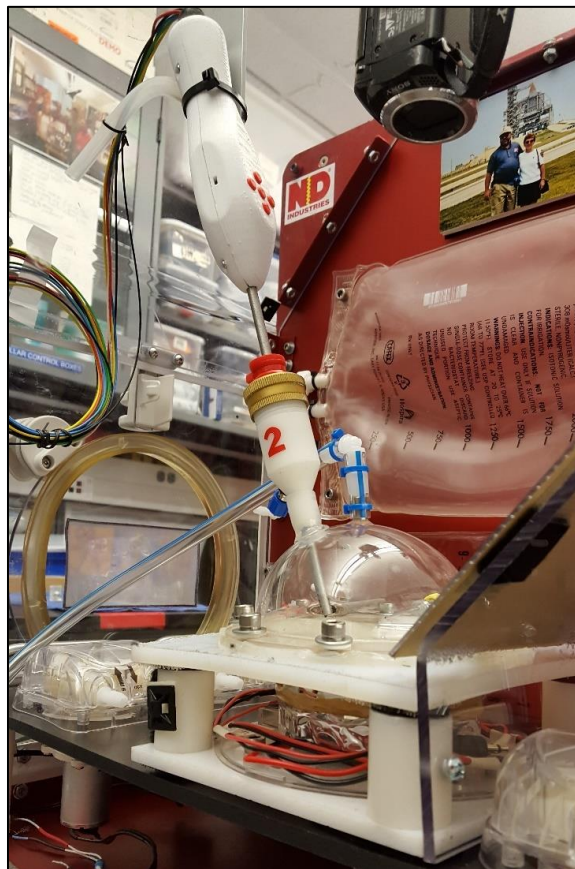
Figure 2 – UofL Aqueous Immersion Surgical System

<u>2.4.1.1 Surgical Immersion Dome</u>

The surgical immersion dome is a transparent, polycarbonate chamber placed over the site of a wound. Figure 3 (left) depicts a SolidWorks (V17, Dassault Systèmes, Waltham, MA) rendering of the surgical immersion dome and Figure 3 (right) shows the dome placement on a human abdomen. It prevents contamination of the spacecraft with blood and/or tissue debris, reduces intraoperative blood loss, provides a sterile microenvironment, and maintains visualization of the operative field [1]. The immersion dome features endoscopic-style trocar ports that allow for instrument exchange and manipulation while maintaining pressure. The hemispherical shape allows the compartment to fill with saline completely without the generation of obstructive air bubbles that potentially distort the visualization of the surgical field [1]. Previous studies have optimized the design of the dome and verified the maintenance of visualization during a hemorrhage situation in a microgravity environment [1]. Future work with the dome involves optimizing the dome to skin-interface with the contour variability of the body.

Figure 3 - Rendering of the polycarbonate dome surgical containment dome (left); dome placement on a human abdomen (right)

2.4.1.2 Leak-Free Trocars

In order to interface with ports on the surgical immersion dome, endoscopic trocars were re-engineered to minimize internal leakage. Figure 4 shows a solid model of the third-generation trocar design. Traditional endoscopic trocars have a tolerated leakage while creating a near-constant CO_2 pressure of 15 mmHg during laparoscopic surgeries but are incapable of preventing substantial internal leakage during saline pressurization of 60-80 mm Hg used during arthroscopic surgery. By using two multi-leaflet valves (Karl Storz) and a dual-tapered diaphragm end cap seal, leak-free trocars can maintain pressure up to 100 mmHg for both air and fluid insufflation.
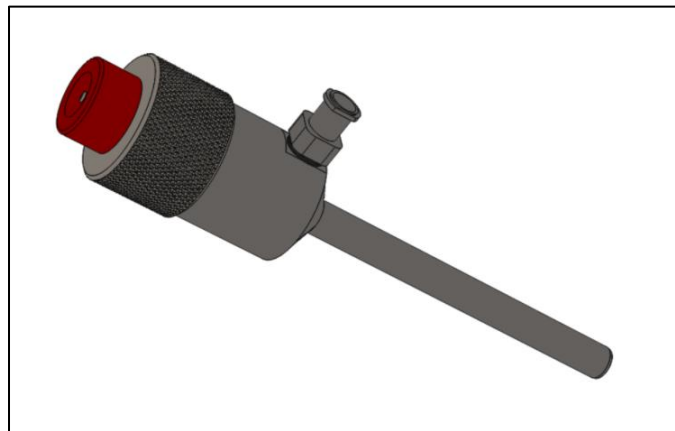
Figure 4 – Solid model of the third-generation leak-free trocars

2.4.1.3 Fluid Management System

The development of an electronic fluid management system is intended to control the various flow functions of the AISS. This system directs the filling and emptying of saline and purging of debris from the surgical immersion dome via the coordinated action of pumps and valves. Continuous input from accelerometers and pressure, flow, and optical sensors provide additional

measurements for system control. A fully-functional fluid management and appropriately sized surgical domes will provide a compact and efficient method to perform surgery during space travel.

Currently two different versions of the fluid management system are being evaluated. Researchers at Carnegie Mellon University are developing a compliant version of the surgical dome incorporating a Raspberry Pi microprocessor. The University of Louisville's version includes a rigid dome and a National Instruments myRIO microprocessor (myRIO-1900)

2.4.1.4 Suborbital Flight Payload Container

All components of the AISS (both the University of Louisville and Carnegie Mellon University flight experiments) are housed in a custom-designed suborbital flight payload container (i.e. custom glovebox). The glovebox is the equivalent to the size of two stacked International Space Station (ISS) stowage lockers (18.5" x 23" x 21.5"). The most recent assembly of the suborbital flight payload container is pictured in Figure 5. The load-bearing components that interface with the payload mounting plates on the SpaceShipTwo are made from 6061 aluminum that was passivated via anodization. The canopy is made from transparent polycarbonate. Each flight experiment is fixed to a 10" x 17" mounting board inside the glovebox.

The glovebox features side doors that hinge downwards for experiment installation, servicing, and removal. There are three pairs of arm access ports, each permitting interaction with the experiment by investigators during the

Figure 5 - Suborbital glovebox with polycarbonate canopy, incubator-style arm access ports, and absorbent liners situated underneath the two modular experiment boards

parabolic and/or suborbital test flights. External electrical connections on the front of the glovebox allow for power distribution to the two experiments via cable feed-through ports. The glovebox has undergone numerous design reviews and changes to ensure proper installment into the spacecraft and containment of the experiments.

2.1.4.5 Modular Experiment Board

Two modular experiments boards are housed inside of the glovebox. One experiment, developed by Carnegie Mellon University, uses a compliant dome that is adhered to the "skin" of a mannequin arm via an elastic strap. The second experiment, developed by the University of Louisville, uses a rigid, transparent dome fastened to a simulated abdominal wall with bolts in a circumferential flange (Figure 6). Both experiment boards house fluid management systems that

control the immersion fluid functionality used in both surgical immersion dome approaches (i.e. rigid and compliant). As the logistics of restraining surgical hardware is critical in low-gravity environments [12, 21, 23], instruments and related components are secured to the board using hook and loop fasteners (Velcro®) and bolts.

The UofL experiment has mechanical and electrical components mounted both above and below the board. Each fluid function is controlled by the myRIO microprocessor. Two peristaltic pumps are used to control filling and emptying of the surgical dome. An infrared LED and optical sensor help regulate the filling function. Two other pumps provide suction and irrigation for the MFSD. A micro-dosing peristaltic pump is included to regulate dome pressure by infusing or withdrawing small volumes of fluid. In addition, this pump injects analog blood to simulate bleeding from the wound-site.
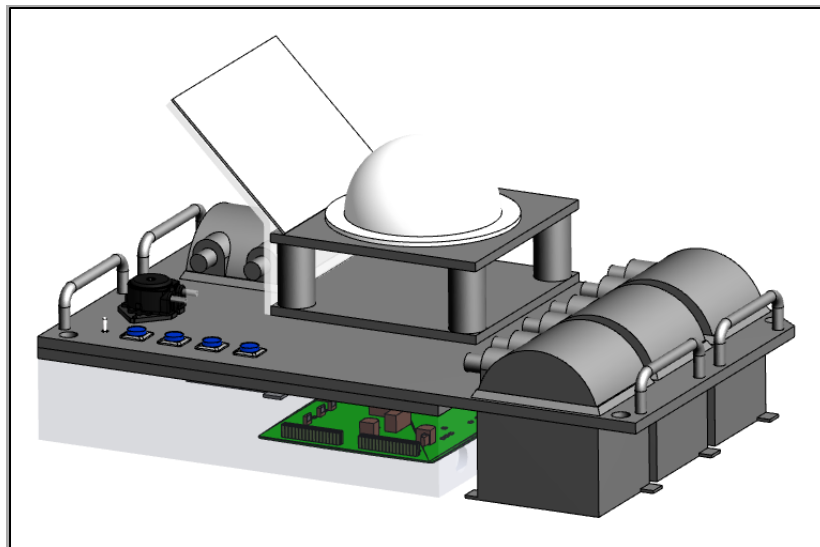
Figure 6 – Solid model of the UofL modular experiment board

2.5 Existing Technologies

Most surgical devices are single-function by design (e.g. isolated suction, irrigation, or cautery). There are few multifunctional surgical technologies currently on the market. One device is the Ethicon, Inc. ENDOPATH® Electrosurgery PROBE PLUS® II. This device, shown in Figure 7, combines suction, irrigation, and monopolar cautery functionality in a 5mm diameter shaft for laparoscopic use. Two handle designs are available: pistol-grip and pencil-grip.
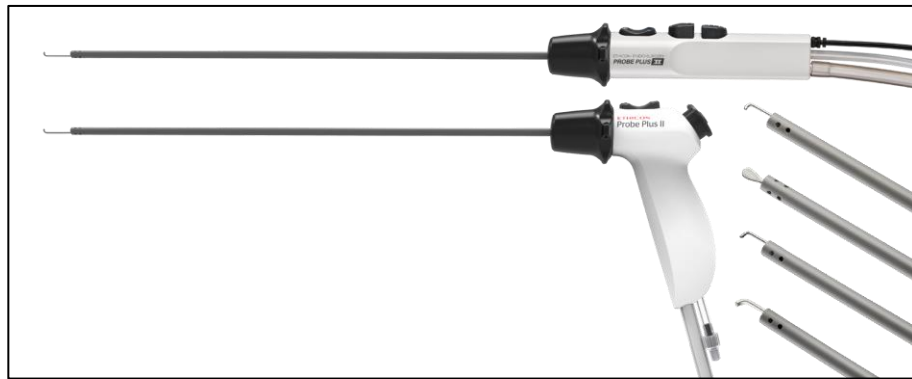
Figure 7 - ENDOPATH® Electrosurgery PROBE PLUS® II

A second multifunctional laparoscopic device was developed by Bovie, Inc. The Bovie Suction Coagulator family (Figure 8) includes laparoscopic devices that combine suction and monopolar cautery.

Figure 8 – Bovie Suction Coagulators

A third multifunctional device was created by Medtronic, the Aquamantys MPR Bipolar Sealers (Figure 9). This device combines irrigation, illumination, and bipolar cautery. Because of the curved shape of the end-effector, this device is only compatible for open surgical procedures.

Figure 9 - Aquamantys MBS Bipolar Sealers

A review of existing surgical technologies highlights the need for more comprehensive endoscopic devices. There is a need for enhanced functionality that integrates suction, irrigation, illumination, visualization, and cautery in a laparoscopic compatible device. Further, miniaturization of current technologies is needed.

2.6 Problem Statement

In recent years, the development of new endoscopic (i.e. laparoscopic, arthroscopic) surgical technology has increased considerably [24-26]. Common examples include dissectors, graspers, cautery scissors, and suction/irrigation devices [27]. Most current endoscopic devices are single-function by design and

16

require frequent instrument exchange during the procedure, increasing the overall procedure duration [28, 29].

Studies approximate that 10-30% of the total procedure time is allocated to instrument exchange [30]. This can significantly disrupt surgeon focus, potentially compromising patient safety [27, 31, 32]. Interestingly, laparoscopic instruments are frequently used for numerous tasks in addition to their primary function [28]. For instance, a suction instrument may be used temporarily as a tissue retractor to move tissue/organs.

While existing endoscopic hardware configurations are unfit for surgical procedures in space, there is opportunity to improve their effectiveness for surgical procedures on Earth. Correspondingly, miniaturization and consolidation of endoscopic technology is necessary considering the limited space and materials and crew on a spacecraft [12]. Advances in endoscopic hardware will require smaller and more flexible end-effectors that can accomplish more than one task [28].

As NASA is planning for longer space explorations, the need to perform surgery in a safe, sterile, and efficient manner while in a spacecraft or colony will continue to grow. Given the limited time, material resources, and crew in space, economy and efficiency during surgical procedures are critical. The development of the Multifunctional Surgical Device addresses this limitation and is being prepared for an in-flight performance evaluation during the suborbital flight campaign planned for late 2018.

Recent flight experiments have demonstrated various surgical capabilities in space. Considering the potential surgical needs on a space flight, five functions have been identified to improve surgical efficiency: suction, irrigation, illumination, cautery (cut and coagulation), and visualization. Incorporation of these five functions into a single device will also offer time and cost-saving advantages to surgeons in Earth-based surgical procedures.

To support the University of Louisville's Astrosurgery research, the multifunctional device should be small, hand-held, and AISS compatible. The shaft of the instrument must be durable, leak-free, and compatible with the leak-free trocars. The fluidics and electronic controls should interface with the AISS Fluid Management System, as pressure/volume regulation inside the dome is critical.

By developing a Multifunctional Surgical Device compatible with the surgical isolation domes, future surgeries performed in the microgravity environment will have increased efficiency and control of the operative field to provide a safe and sterile environment for both the patient and crew members.

2.7 Capstone Project Developments

2.7.1 Project Scope

In Fall 2016, an undergraduate Bioengineering Capstone design group worked on an early concept of the Multifunctional Surgical Device. The first proof-of-concept device included suction, irrigation, and illumination functionality.

<u>2.7.2 Design Intent</u>

To help illustrate the device concept, the "Astrosurgery" team provided

UofL researchers with a rendering (Figure 10) of a modified Medtronic DLP

Cardiac Suction wand and a five button "remote-control configuration". This

mock-up design captured the compact endoscopic configuration that the group

envisioned.
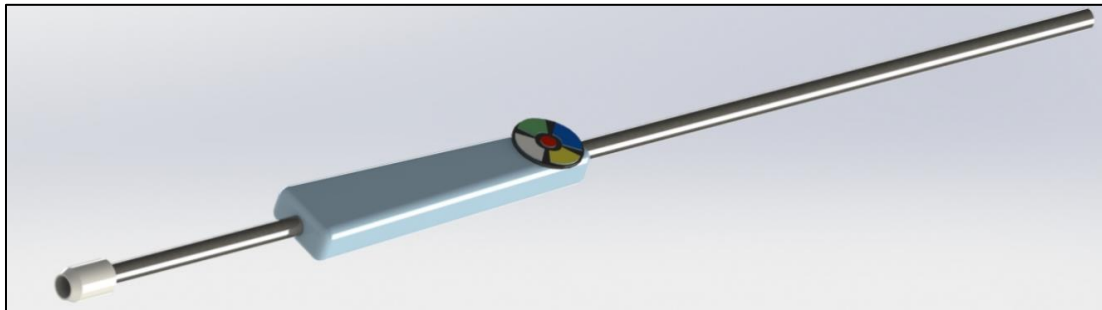
Figure 10 - Initial rendering of MFSD that includes a mock-up of a Medtronic
DLP Cardiac Suction wand with a five-button "remote control-like"
configuration

When developing design criteria for this project, time was a significant

constraint. Before beginning the design process, the team developed a Pugh

Matrix to help identify the most critical functions, as outlined in Table 1. While the

Astrosurgery team was interested in combining five functions: suction, irrigation,

illumination, cautery (both cut and coagulation), and visualization, the team

recognized the short project timeline. To evaluate the importance and feasibility

of each potential function, team members considered potential product selections

(of 2, 3, and 4 functions). The potential designs were compared to the existing

Medtronic DLP Cardiac Suction Wand. Based on the results, the team decided to

focus on three functions: suction, irrigation, and illumination.

Table 1 - Pugh matrix for development of Prototype I

Pugh Matrix				
	"S" - Same	"+" - Better	"-" - Worse	
Evaluation Criteria	Medtronic DLP Cardiac Suction Wand	Suction / Irrigation Wand	Suction / Irrigation / Illumination Wand	Suction / Irrigation / Illumination / Electrocautery Wand
Reasonable Cost (10%)	S	-	-	-
Functionality (30%)	S	"+"	"+"	"+"
Ergonomic Design (10%)	S	S	S	S
Safety (30%)	S	S	S	-
Usability (20%)	S	"+"	"+"	"+"
Total +	-	0.5	0.5	0.5
Total -	-	0.1	0.1	0.4
Total Score	-	0.4	0.4	0.1

2.7.3 Device Development

2.7.3.1 Mechanical Design

Development of the three-function (suction, irrigation, and illumination) device began in late September of 2017 and concluded in early December of that same year. Specific tasks involved in device development included: 1) the selection of components that provided each functionality; 2) the mechanical design and fabrication of a housing that incorporated all necessary components; and 3) the design and development of an electronic control system for benchtop testing.

Figure 11 illustrates the general components of the MFSD and fluidic control system. At this stage, the fluid pathway included one peristaltic pump (Adafruit, 1150) and two one-way solenoid valves (Electric Solenoid Valves, RSC-2-12V). As suction and irrigation shared the same fluid channel in the device, the singular pump would also regulate both functions by running in the clockwise and counterclockwise directions as needed. To maintain pressure in each fluid line, two one-way solenoid valves were placed downstream of the y-connector that split the suction and irrigation fluid lines. Finally, the suction and irrigation lines were connected to saline and waste reservoirs, respectively.

The handle design was composed of two halves that formed a clamshell-like assembly. This housing integrated five pushbuttons, a fiber optic cable, and a suction wand (Karl Storz, Suction and Irrigation Tube, 26172BN). The distal end of the device included a 6mm opening to allow for the 5mm Karl Storz shaft and
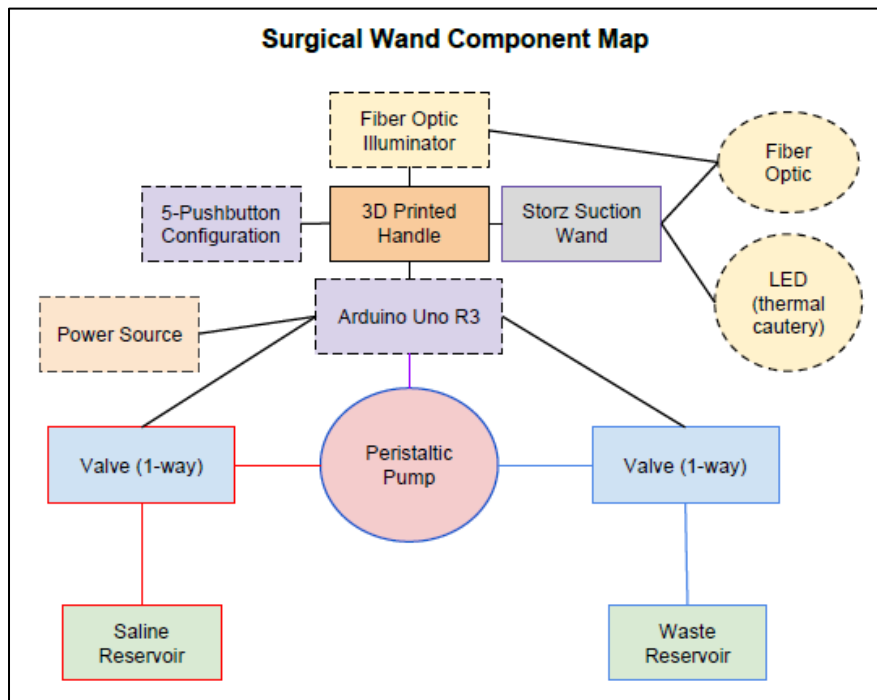
Figure 11 - Component map for Prototype I

1 mm fiber optic. On the proximal end, there were two openings: a smaller diameter hole for ⅜" silicone tubing and a larger ½" diameter hole for a wire-bundling component. The bottom clamshell included placements for the smaller and larger diameter portions of the Karl Storz Suction Wand shaft. To provide illumination, a 1.0 mm cladded fiber optic cable (Mitsubishi Rayon Co. LTD, SH1001-1.0) was adhered to the outer diameter of the Karl Storz Suction Wand with electrical tape. One end of the cable was connected to a 1.5 W LED (Raysell, Super Eska™ Polyethylene Jacketed Optical Fiber Cord, PMMA 005), while the other end provided localized illumination at the tip of the device.

The final proof-of-concept design (Design I) is shown in Figure 12. The overall shape of the handle was designed for thumb-activation. The top clamshell had 12 mm cutouts for the five pushbutton configuration. The center button activated illumination, the upper button activated suction, and the lower button activated irrigation. The left and right buttons controlled cutting and coagulation
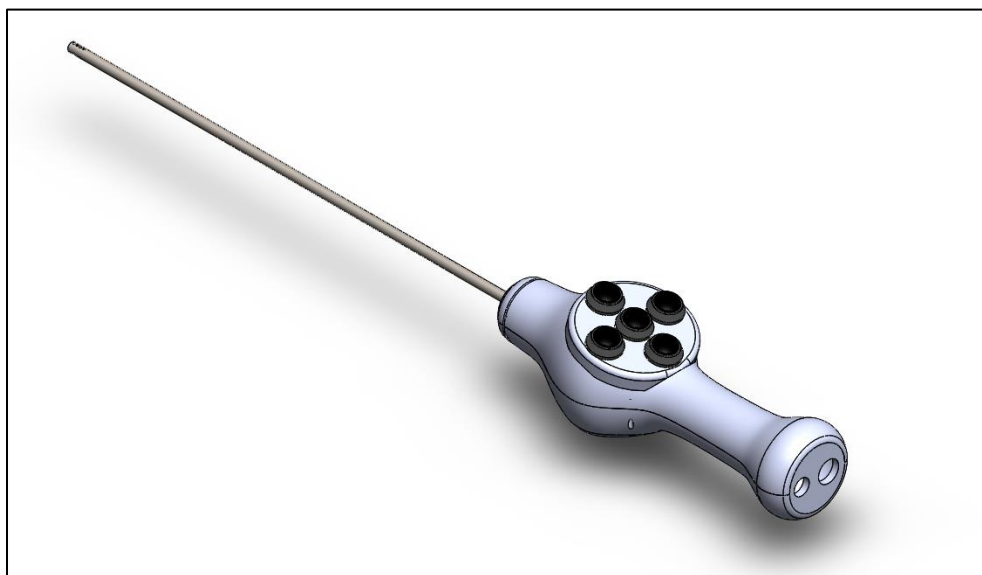
Figure 12 – Solid model of Design I

functions (simulated via LED indicators). Finally, small holes for #4-40 set screws

were located on the clamshells for device closure.

2.7.3.2 Electronic Design

To demonstrate device functionality, a stand-alone control circuit (Figure

13) was developed on a National Instruments ELVIS breadboard. The system
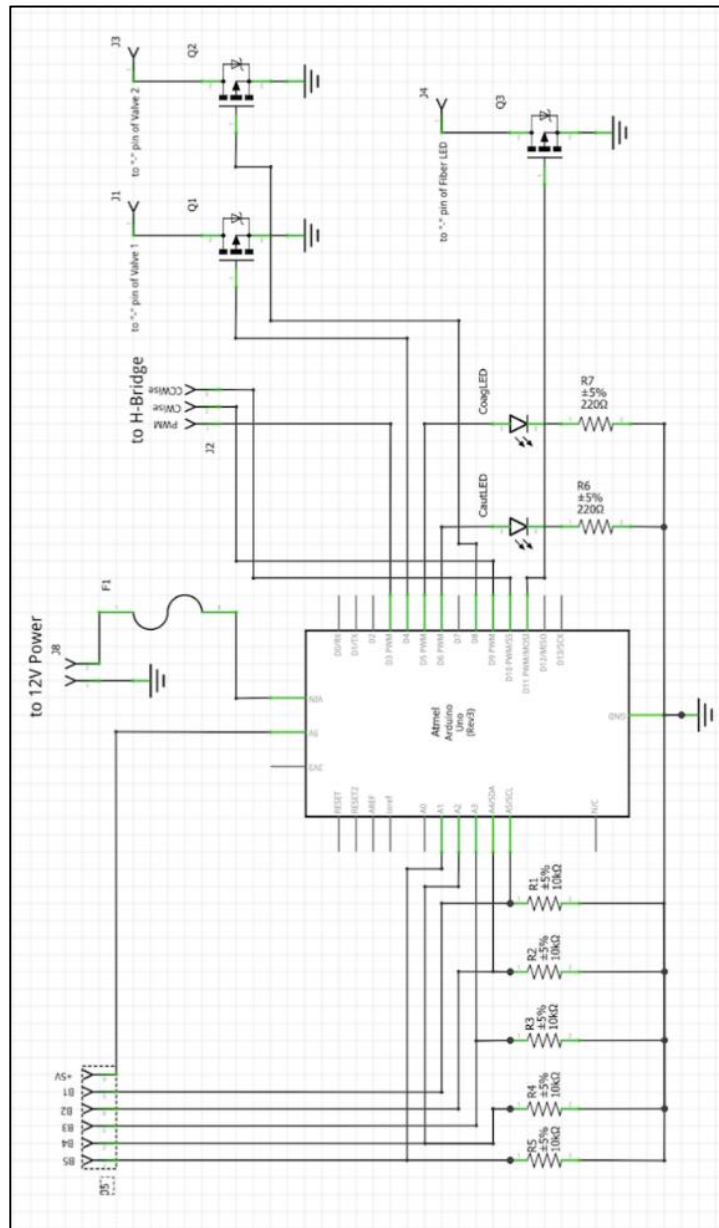
Figure 13 - Circuit control schematic for Prototype I with Arduino UNO (Rev 3)

23

utilized an Arduino™ UNO Rev 3 as the control microprocessor. A series of state-change functions created using the Arduino™ IDE were developed to enable momentary activation of each function.

2.7.4 Prototype I Review

The clamshell design of Prototype I was fabricated using additive manufacturing (i.e. 3D printing, specifically FDM, Fused Deposition Modeling) with Zortrax-ABS material. Following the fabrication of the clamshell device, the device components were secured in place and fluid components were connected according to Figure 11. The assembled prototype is shown in Figure 14, while Figure 15 shows the fluidics setup as utilized during device testing. The proof-of-concept device was successful in providing suction, irrigation, illumination, and LED-represented cautery.

Figure 14 - Assembled Prototype I

A review of the first prototype was conducted following the completion of the Capstone project. Four student reviewers from the Astrosurgery project evaluated the device in terms of each function (suction, irrigation, illumination), ergonomics, assembly, and fluid/electrical setup. Table 2 outlines the results of the survey. Illumination received the lowest score, as the fiber optic was too small to provide adequate lighting. The second lowest category was ergonomics,
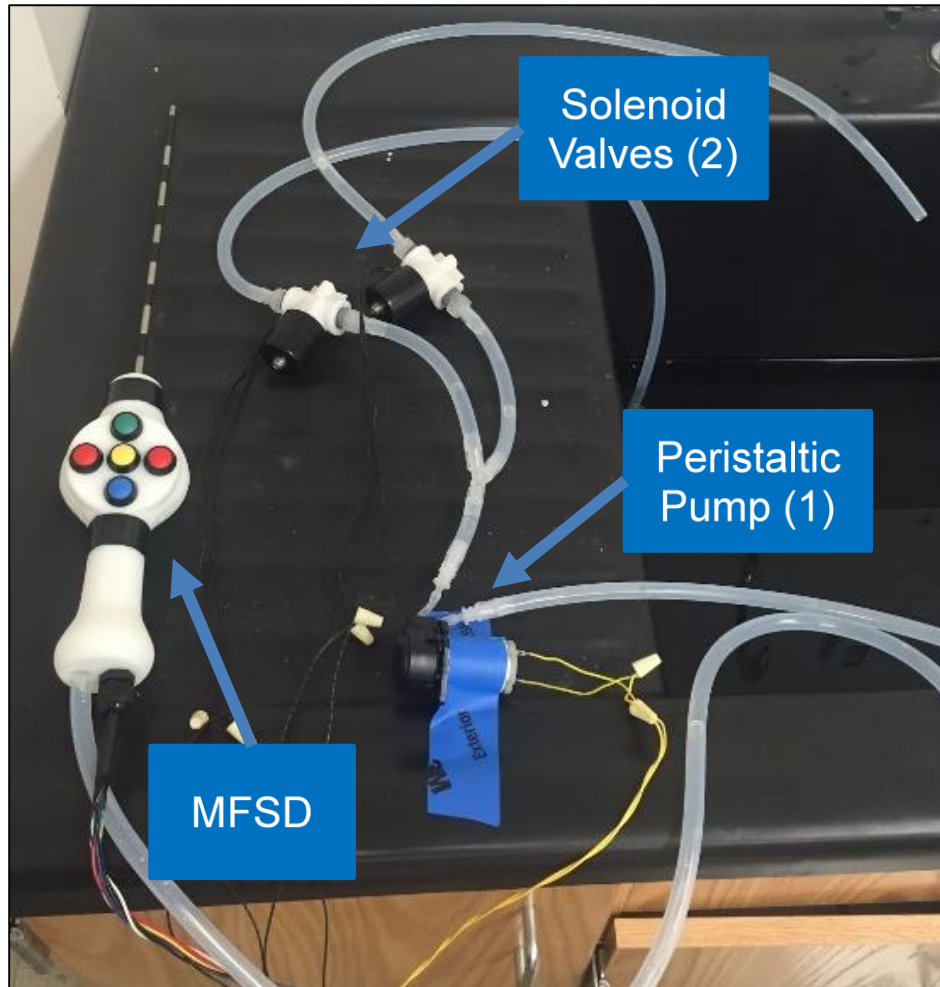
Figure 15 - Fluidics setup for verification of Prototype I functionality

as the device was developed for thumb-activation of functions. After reviewing

the device, the Astrosurgery team determined that index-finger activation would

maximize surgeon comfort. Finally, it was determined that suction and irrigation

functionality needed improvement. Flow rates in the proof-of-concept device

were capable of reaching 1 mL/sec but were incapable of reaching thresholds

suitable for endoscopic procedures (i.e. 1 L/min).

Table 2 - Design review of proof-of-concept device (Prototype I)

Evaluation Criteria	Reviewers				Average Score	Score	Description
	A	B	C	D			
Suction Function	2	2	2	4	2.50	1	Poor
Irrigation Function	2	2	3	4	2.75	2	Fair
Illumination Function	1	1	2	2	**1.50**	3	Adequate
Ergonomics	2	2	1	3	**2.00**	4	Good
Button Configuration	2	3	4	1	2.50	5	Excellent
Device Assembly	3	3	1	1	2.00		
Fluid System Function	4	3	4	3	**3.50**		
Electrical Setup	4	4	3	3	**3.50**		

III. MATERIALS & METHODS

3.1 Design Criteria

Several design criteria (essentially the project design and technical objectives) were established at the beginning of the project. These helped guide the development and testing of the MFSD.

3.1.1 Design Objectives

Table 3 summarizes the design objectives and their rank/relative weight. Three categories of design objectives were established: *performance, usage, and other*. Initially, each design objective was ranked (1 = not important; 5 = extremely important) and then the relative weight was calculated. The *performance* criteria include the following: 1) The device provides adequate suction/irrigation rates; 2) The device provides adequate localized illumination; and 3) The device interfaces with a control circuit. As these are the main functions of the device, all performance objectives are "extremely important".

The *usage* criteria include the following: 1) The device is easy to assemble; 2) The device handle is ergonomic; 3) The button-activation is accurate and comfortable for the user; 4) The device is lightweight; 5) The device is reliable; and 6) The device is reusable. Reliability/reusability are "very important", as the user must be confident that each function performs

Table 3 - Design objectives for the MFSD

Design Objectives	Category	Rank	Relative Weight	Score	Rank
Adequate suction/irrigation	Performance	5	12.20	1	Not important
Adequate illumination	Performance	5	12.20	2	Slightly important
Easy to assemble	Usage	3	7.32	3	Moderately important
Compatible with control circuit	Performance	5	12.20	4	Very important
Ergonomic handle design	Usage	4	9.76	5	Extremely important
Comfortable button-activation	Usage	3	7.32		
Low cost	Other	1	2.44		
Lightweight	Usage	2	4.88		
Reliability	Usage	4	9.76		
Reusable	Usage	4	9.76		
Leak-free/water proof	Performance	5	12.20		

consistently upon activation and for the intended duration. Ergonomics is also
"very important", considering the feedback received from the proof-of-concept
device review. Ease of assembly and comfortable button activation are
"moderately important", but not critical to the project success. It is important,
however, that the button activation should not be so easy (i.e. requiring little
force) that the user may accidentally activate a function. Finally, the low-weight
objective is "slightly important".

The only design objective in the *other* category is 1) The device should be
low cost. While cost will become more important as the project progresses, it is of
minimal importance during the prototyping phase.

<u>3.1.2 Technical Specifications</u>

In addition to the qualitative guidelines established from the design objectives, technical specifications were also developed. Table 4 outlines the technical specifications and their target values/trends. These provide quantitative values (or trends) for a variety of the design objectives. The technical specifications include the following: 1) device weight (lbs); 2) device length (in); 3) device diameter (in); 4) fluid (i.e. suction, irrigation) flow rate (mL/min); 5) illumination (lux); and 6) button activation force (lbf).

Device weight and diameter should be minimized (while still comfortable in most hands) to reduce overall size and material cost. In addition, a more compact device is advantageous, given the limited space on stowing equipment and supplies on a spacecraft. Illumination should be maximized to provide enhanced local visualization. Considering the constraints of the payload container interior volume for evaluation missions, device handle length should be kept near five inches to permit usage through the arm access ports. Finally, fluid flow rate should reach 1 L/min to be consistent with current endoscopic flow rate practice.

Table 4 - Technical specifications for MFSD

Technical Requirement	Direction of Improvement	Target (if applicable)	Direction	Symbol
Device weight (lbs)	▼		Minimize	▼
Device length (in)	X	5 in	Target	X
Device diameter (in)	▼		Maximize	▲
Fluid flow rate (mL/min)	X	1 L/min		
Illumination (lux)	▲			

<u>3.2 Device - Hardware</u>

<u>3.2.1 Fluid Components</u>

<u>3.2.1.1 Fluid Schematic</u>

The MFSD fluid system (Figure 16) began with a single fluid channel (Cole Palmer, 3/8" OD / 1/4" ID silicone tubing, # EW-95802-05) that exited the proximal end of the wand. The fluid line divided into two separate flow paths via a Y-shaped connector (Cole Palmer, EW-40726-45). One side of the fluid line then connected to a peristaltic pump for control of suction, while the other side connected to a second peristaltic pump for irrigation control. The use of two dedicated peristaltic pumps eliminated the need for valves, as peristaltic pumps are occlusive and can maintain pressure within the fluid line. Finally, the opposite
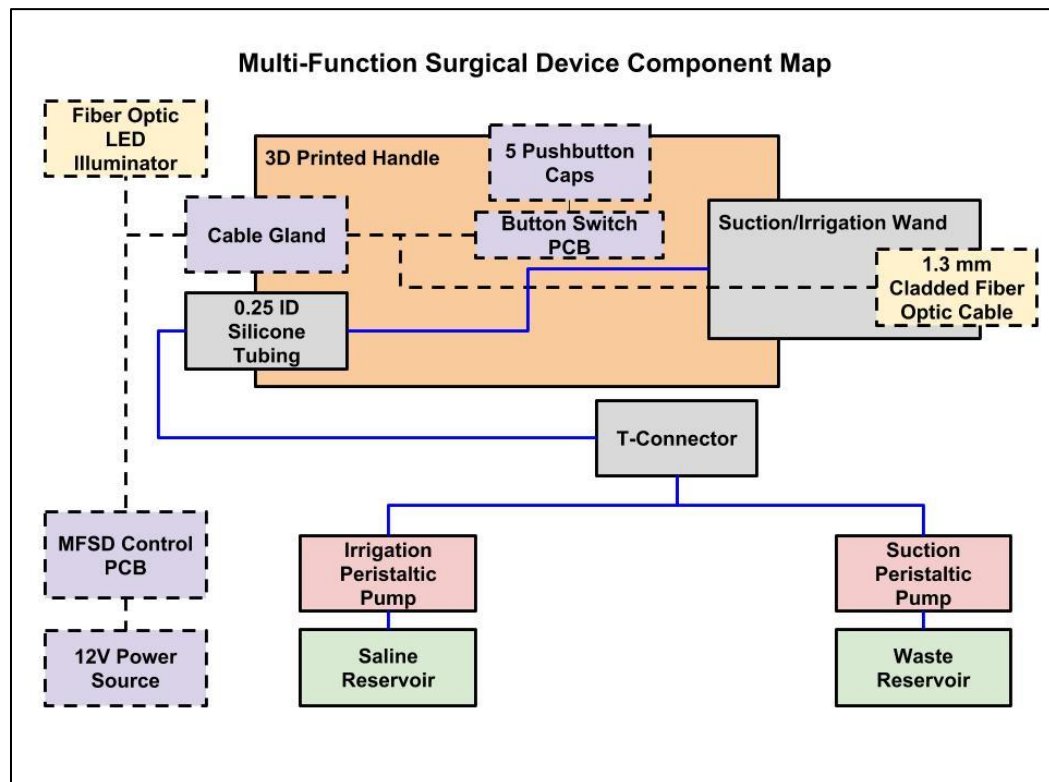
Figure 16 - Component map for the MFSD

end of each pump connected to an irrigation fluid (e.g. saline) reservoir and waste fluid collection reservoir, respectively.

3.2.1.2 Peristaltic Pumps

The new fluid system utilized two peristaltic pumps to control the suction and irrigation lines. The removal of solenoid valves reduced the total number of fluid components from four in the proof-of-concept design to three in subsequent prototypes.

Flow rates for endoscopic surgical procedures should be able to reach 1 L/min; therefore, peristaltic pumps for this project should reach similar thresholds. 12V DC enclosed peristaltic pumps (Honline Industrial Co. Ltd., China) were selected for the fluidics system (Figure 17). These pumps provide a precise bi-directional (CW/CCW) flow rate of 1 +/- 8% L/min flow rate [33]. The PharMed BPT® Tube meets USP Class VI, FDA, and NSF criteria, and easily interfaces with 5.5mm(ID) external tubing via polypropylene barbed fittings
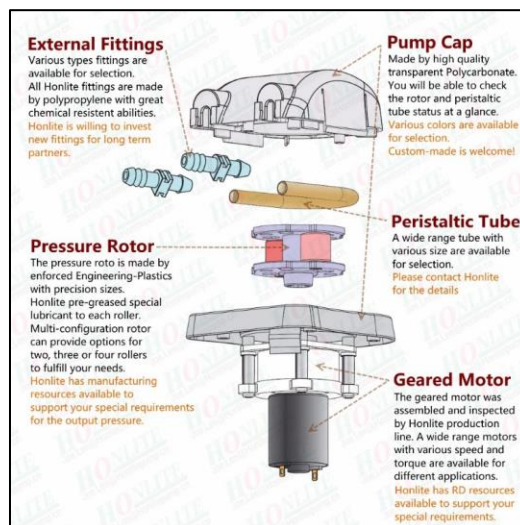
Figure 17 - Overview of Honlite 1 L/min Peristaltic Pump [33]

3.2.2 Button Switch Configuration

The button switch configuration in the proof-of-concept device needed significant improvement. While the pushbuttons were reliable and comfortable to activate, they were too large and contributed greatly to the device diameter. In an effort to reduce the overall device size for better ergonomics, a more compact option was fabricated using five button switches (E-Switch, TL1105EF250Q7.3RED, EG1832-ND) soldered to a custom printed circuit board (PCB). This allowed for compact and simple installation via attachment to the top clamshell.

3.2.2.1 Circuit Schematic

A custom instrumentation circuit was developed to control each device function using five button switches. Each connected to a common 5V power source on one side and to five individual signal pins on a 1x6 header on the other. This configuration permitted connection to an integrated control system during later device development. Figure 18 shows the Multisim (National Instruments, Austin, TX, V14.1) schematic of the button switch configuration.
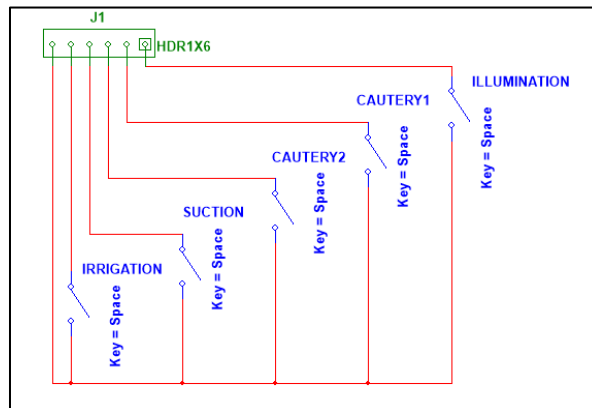
Figure 18 - Circuit schematic for PCB of five button switch configuration

The circuit schematic provided the physical connections of components for a custom printed circuit board (PCB). Ultiboard (National Instruments, Austin, TX, V14.1) was used to position all parts and connections on a two-layer, FR4 circuit. The board outline for Design 1 (Figure 19) was circular with a 1.1" diameter. The button switch configuration PCB design featured button switches in configuration similar to a "plus" sign (+). While this geometry is significantly smaller than the button switch configuration in the proof-of-concept device, further consolidation was considered. For this reason, Design 1 was not submitted for production.
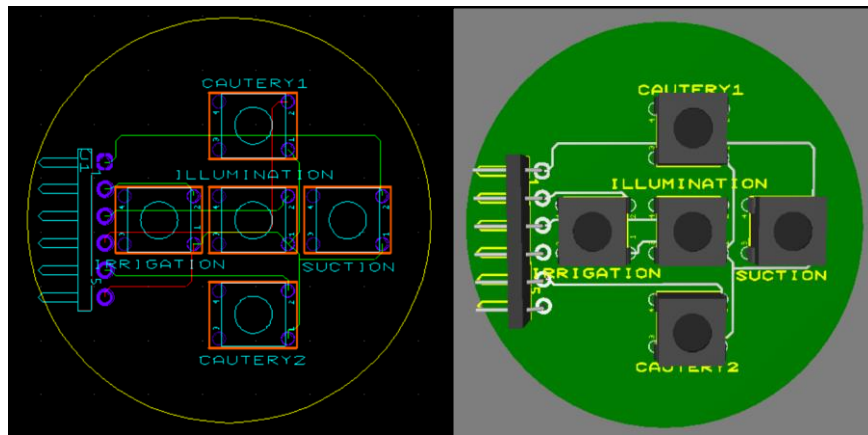
Figure 19 - 2D schematic and 3D model of PCB Design 1 (circular)

3.2.2.3 PCB Design 2

In effort to reduce the board geometry (i.e. to reduce the overall device diameter), Design 2 (Figure 20) was created with a "rounded-rectangular" board outline. This 1.4" x 1.0" outline reduced the width of the PCB while maintaining adequate spacing between each button switch (0.35" center-to-center). In addition, 0.125" diameter through-holes were added to accommodate #4-40

screws that assisted in mounting the PCB to the inner surface of the top

clamshell. All component selections from Design 1 were maintained in Design 2.
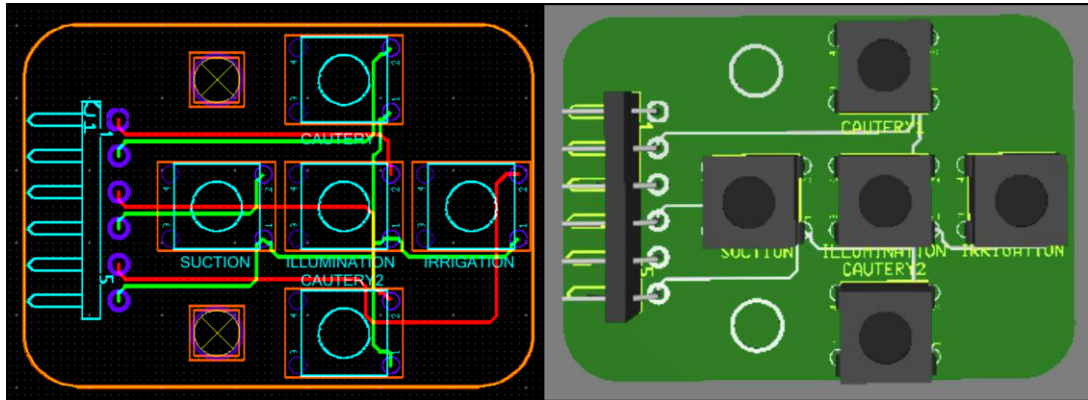
Figure 20 - 2D schematic and 3D model of PCB Design 2 (rounded
rectangular)

Seeed Studio Fusion [34] was used to fabricate PCB Design 2. All

components were soldered to the PCB via through-hole soldering according to

the schematic. These button switches had an actuator height of 7.3 mm. After

installing the PCB into the top clamshell, the actuator was designed to protrude

out from the outer surface to permit finger-tip activation. A 6-pin, right-angle,

rectangular male header (Molex, 0022053061, WM4304-ND) was mounted to the

posterior end of the PCB and mated to a 6-pin rectangular female connector

(Molex, 0022012067, WM2015-ND). This provided a connection to the control

system later in device development.

 3.2.2.4 Silicone Button Pad

While the button switches mounted on the PCB provide audible activation,

they are small in diameter and uncomfortable to activate with the index finger.

For this reason, a button interface was designed to fit on top of the five button

switches. The button pad layout was designed to resemble the "plus" sign (+) configuration of the button switches. The button pad fit securely over the actuators and protruded out of the top clamshell for index finger device actuation, effectively increasing the button surface area to 0.25". This cap also created a barrier to water leakage that may interfere with the device electronics. A negative mold (Figure 21) of the button pad was created to allow for fabrication using two-part silicone rubber. The negative mold was filled with slow-setting two-part silicone rubber (Smooth-On Inc., Mold Star™ 15 SLOW) to fabricate the component.
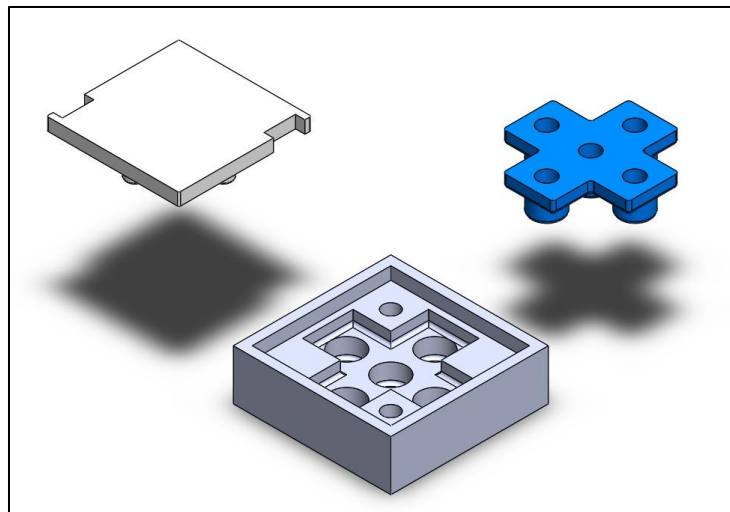
Figure 21 – Solid model of button pad and negative mold

3.2.2.5 Pushbutton Caps

To provide a more comfortable and audible button activation, an individual stand-alone pushbutton cap was designed (Figure 22). Rather than the interconnected design of the silicone button pad, this design featured discrete button caps for each actuation trigger. This helped to isolate each function and
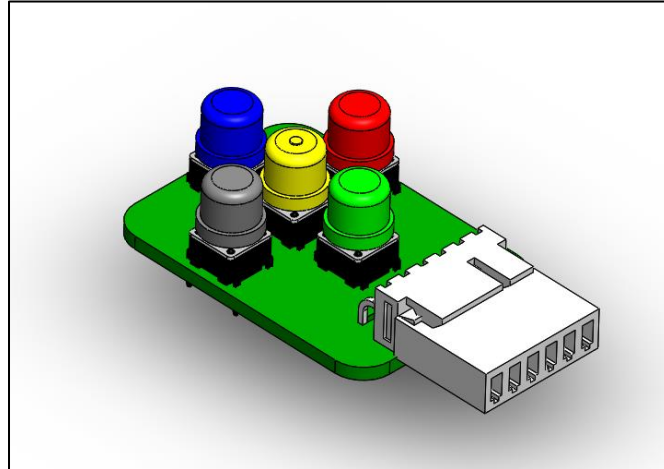
Figure 22 – Solid model of PCB assembly with plastic pushbutton caps

prevent accidental activation of multiple functions (accidental multiple button switch press). This configuration provided visual and tactile cues to help the surgeon distinguish each button's functions. In the model, the blue button towards the distal end of the device activates irrigation, while the green towards the proximal end activates suction. The red button on the left and the black button on the right (from the user's point of view) distinguish cut and coagulation, respectively. The yellow button in the center is for illumination. In addition, the yellow button also features a small, tactile bump that allows the user to determine the "home-position" without relying on the color system. Five pushbutton caps were fabricated with ABS plastic using a FlashForge Creator Pro (FlashForge Corp., China) 3D printer.

3.2.3 Fiber Optics

Illumination for the MFSD is provided by a fiber optic system (Figure 23). A 12V LED illuminator (Raysell, Super Eska™ Polyethylene Jacketed Optical

Figure 23 - 1.3 mm Super Eska™ polyethylene jacketed optical fiber cord

Fiber Cord, PMMA 005) and 1.3 mm cladded fiber optic cable (Mitsubishi Rayon Co. LTD, SH4001-1.3) were selected to provide localized illumination at the tip of the surgical wand. The black cladding around the 1.0 mm core prevents light leakage for optimal illumination.

The distal end of the fiber optic cable was secured within the inner lumen of the metal channel via medical-grade epoxy. The proximal end of the fiber optic was connected to a 1.5 W fiber optic LED illuminator and was secured via a small set-screw.

3.2.4 Suction/Irrigation Wand

The proof-of-concept device used a Karl Storz suction wand for the main fluid channel. While this component was durable and of the correct 5mm outer diameter, there was no clear method of incorporating the fiber optic cable. When the fiber optic cable was adhered to the outer diameter with electrical tape, the device was unable to prevent leakage from the insertion trocar when the AISS dome was pressured with saline to 100 mmHg. To solve this problem, a custom suction wand was designed to provide compatibility with the fiber optic cable. The main 5mm circular geometry and irrigation holes in the Karl Storz suction wand were maintained. A small lumen was added inside the main fluid channel to

Figure 24 – Solid model of suction/irrigation wand distal tip showing dual-lumen design for fluid line and fiber optic cable (lumen outer diameter ~5 mm)

secure the fiber optic cable for localized illumination (Figure 24). By creating a path for the fiber optic *inside* the main channel, the circular geometry of the shaft was maintained and the wand could properly be used with leak-free trocars in the AISS. In addition, the proximal end of the wand featured small, rectangular cutouts that mate with snap-in features on the bottom clamshell (Figure 25).

Proto Labs (Maple Plain, MN) fabricated the first prototype of the suction wand with Accura 60 (SLA) using normal-resolution stereolithography (0.004" layers). Accura 60 has the ability for fine detail printing, provides good stiffness, has a relatively high tensile strength (58-68 MPa) [35]. In addition, this material is transparent which gives surgeons the ability to visualize blockages within the

Figure 25 - Side view of suction/irrigation wand

line. A standard finish was applied to the final product; however, the wand was further sanded down with a gradient of fine sand paper to create a smooth surface finish.

Proto Labs fabricated a second suction/irrigation wand of the same design with normal-resolution direct metal laser sintering (30-micron layers) using 316 L stainless steel (CL 20ES). This material allowed for production of quality metal parts with the fine features, tight tolerances, and resistance to corrosion [36].

3.2.5 Clamshell Handle

The clamshell housing is the main component that the surgeon grips when using the device. In addition, the clamshell handle holds numerous device components including the metal suction/irrigation wand, silicone tubing, the button switch PCB, five 3D-printed pushbutton caps, and a cable gland that passes through the electronic wiring.

Using feedback from the Prototype I review, three subsequent design iterations of the handle were completed. All designs were fabricated with additive manufacturing (i.e. 3D printing) using a LulzBot Taz 6 (Aleph Objects, Inc., Loveland, CO) printer and white nGen filament. nGen, a co-polymer material made with Amphora AM3300, was selected for its strength, dimensional stability, and attractive print finish [37]. Appendix X outlines the printer characteristics and print settings used for the device fabrication with nGen.

3.2.5.1 Design II

In contrast to the thumb-activation style of the proof-of-concept device, design II (and all designs thereafter) featured a comfortable pencil-grip grasp with index fingertip activation. This configuration offered more fine control of the device tip. This design was also significantly smaller in length and diameter than the proof-of-concept device. The clamshell handle for Design II was roughly 6 inches in length 1.6 inches wide (at the widest portion) and is shown in Figure 26. The two clamshells were designed for mating with six (6) #2 x 0.5" self-tapping screws.
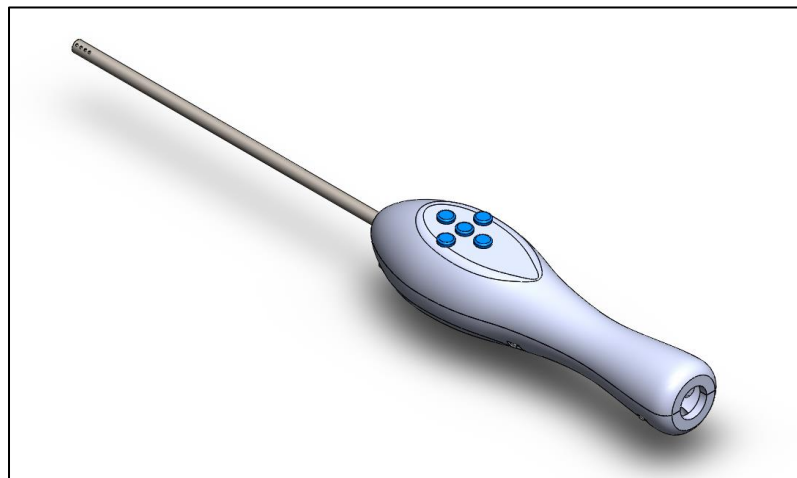
Figure 26 – Solid model of MFSD Design II

3.2.5.2 Design III

While design II featured a large ergonomic improvement, it was difficult to stabilize in the hand with the rounded outer edges. For this reason, the sides of design III were flatter on the sides (where the thumb and middle finger would grasp). Figure 27 illustrates Design III. Length of the clamshell handle did not change; however, the assembly features for the suction/irrigation wand were

moved forward to expose more of the wand. This increase in length was more compatible with the leak-free trocar design. Finally, two of the assembly screws were replaced with snap-fittings.
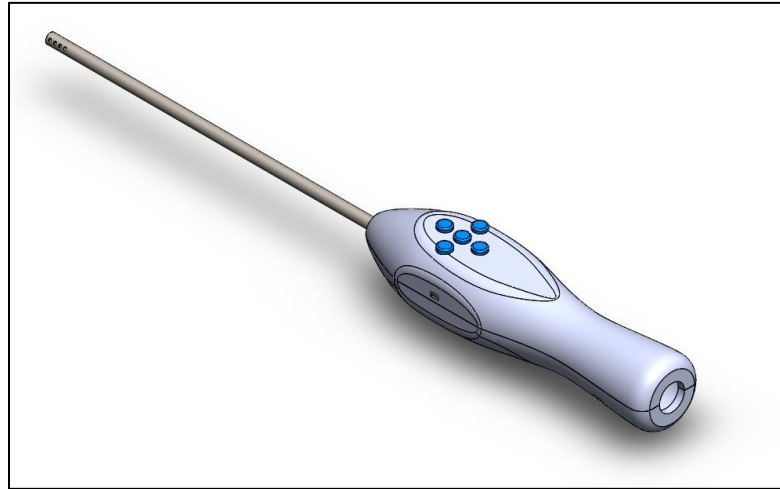
Figure 27 - Solid model of MFSD Design III

3.2.5.3 Design IV

Design IV (Figure 28) represents the final design iteration of the clamshell handle. The length of the handle was reduced to approximately 5 inches. The flattened sides incorporated in Design III were maintained. The smaller diameter (where the device would rest between the thumb and index finger) was reduced by approximately ¼" to improve user comfort when holding the device. The snap fittings were removed and four (4) #2 x 0.5" self-tapping screws were included for assembly. Finally, two new assembly features were added. Small mating lips were added to the outer edges of both clamshell (the top halve hanging over the
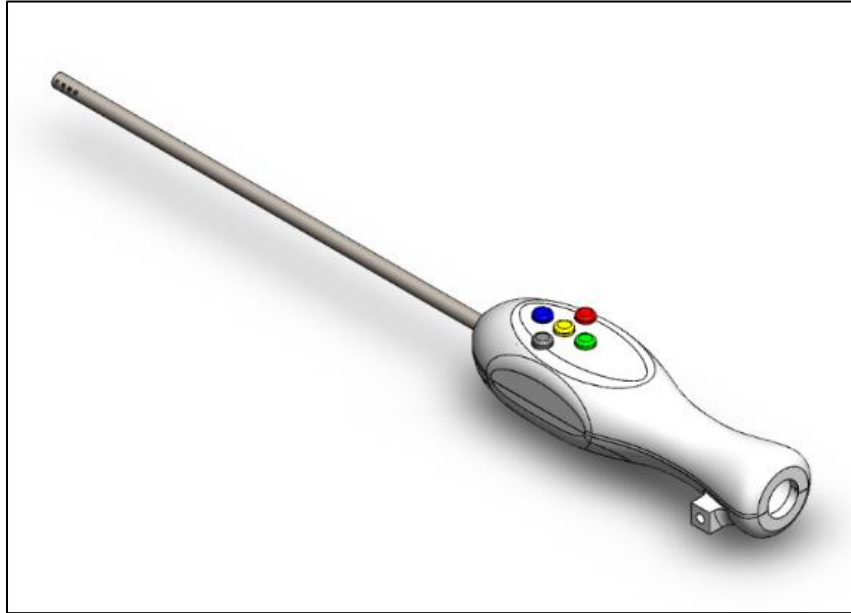
Figure 28 – Solid model of MFSD Design IV

bottom) to prevent water leaks inside the device. Additionally, a small notch was added to the proximal end of the device (left side) for installation into the glovebox. Figure 29 depicts an exploded view of the assembly.
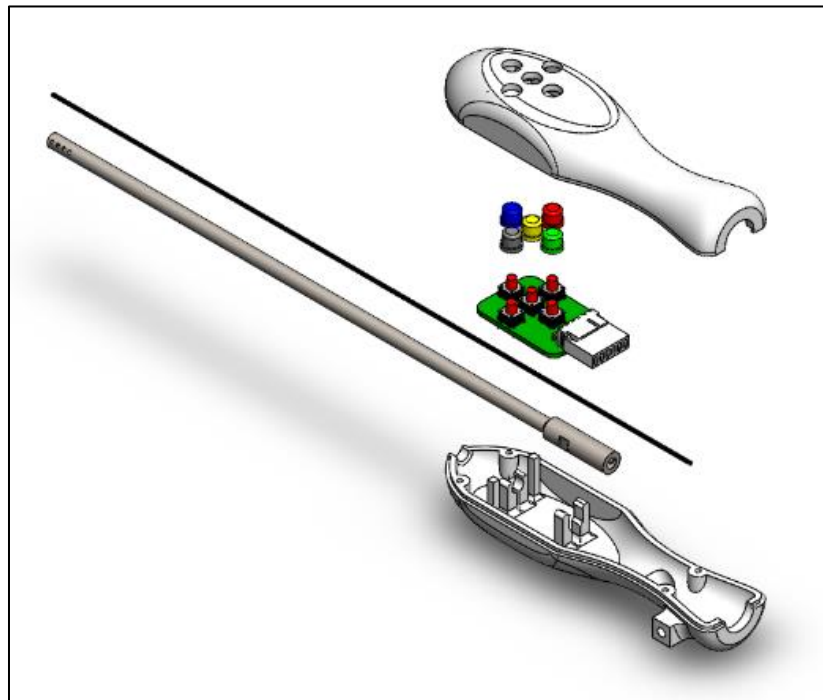
Figure 29 – Solid model of exploded view of Design IV

3.2.6 Stand-Alone Control Circuit

The scope of this project did not permit full integration with the AISS FMS that is still in development; however, verification and validation of device functionality is still necessary. For this reason, a stand-alone control circuit and PCB were developed to allow for benchtop device testing.

3.2.6.1 Microcontroller

An Arduino™ UNO (Rev3) [38] (Figure 30) was selected as the microcontroller for this device. This embedded development platform is based on the Atmega328P microprocessor (Atmel) that provides fourteen digital input/output pins, six analog inputs, a 16Mhz quartz crystal, a USB connection, a power jack, an ICSP header, and a reset button [38].
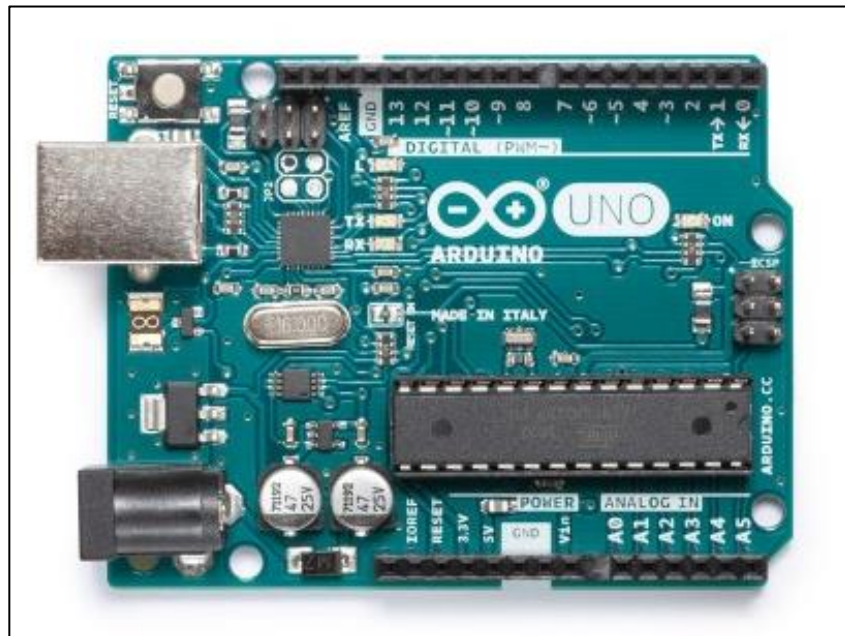
Figure 30 - Arduino™ UNO (Rev3) development platform [38]

3.2.6.2 Circuit Schematic

A custom instrumentation circuit was developed to provide stand-alone control of the MFSD. The schematic of the stand-alone control circuit that established the physical components connections is included in Appendix I.

3.2.6.3 PCB Design

Ultiboard was used to position all parts and connectors on a two-layer, FR4 circuit shield. A "shield" is a PCB layout that is designed to easily interface (i.e. "plug in") to the Arduino™ platform. For purposes of this project, a shield was developed to plug into the Arduino™ UNO (Rev3). Figure 31 shows the 2D and 3D schematics of the resultant PCB shield.

All resistors and LEDs were surface mounted onto the fabricated PCB according to the schematic layout. The capacitor, diode, fuse, and barrel-jack connector were through-hole mounted. Stackable headers were soldered to the PCB to allow the Arduino™ to connect to the pins from below. A 6-pin, vertical, rectangular male header (Molex, 0022232061, WM4204-ND) was mounted to the PCB and mated to a 6-pin rectangular female connector (Molex, 0022012067, WM2015-ND). This allowed for connection to the button switch PCB. To provide inputs for the peristaltic pumps (suction/irrigation), two 2-pin vertical headers (Phoenix Contact, 1755736, 277-1150-ND) were mounted to the board. The larger size of these headers was necessary because of the larger current draw of the pump functionality. In addition, three smaller 2-pin vertical headers (Molex, 22-23-2021, WM4200-ND) were mounted to the PCB. These mated to 2-pin

rectangular female connectors (Molex, 22-01-2027, WM2011-ND) to provide

connections for the fiber optic illuminator and cut/coagulation LED indicators. A

full bill of materials for the stand-alone control PCB can be found in Appendix II.
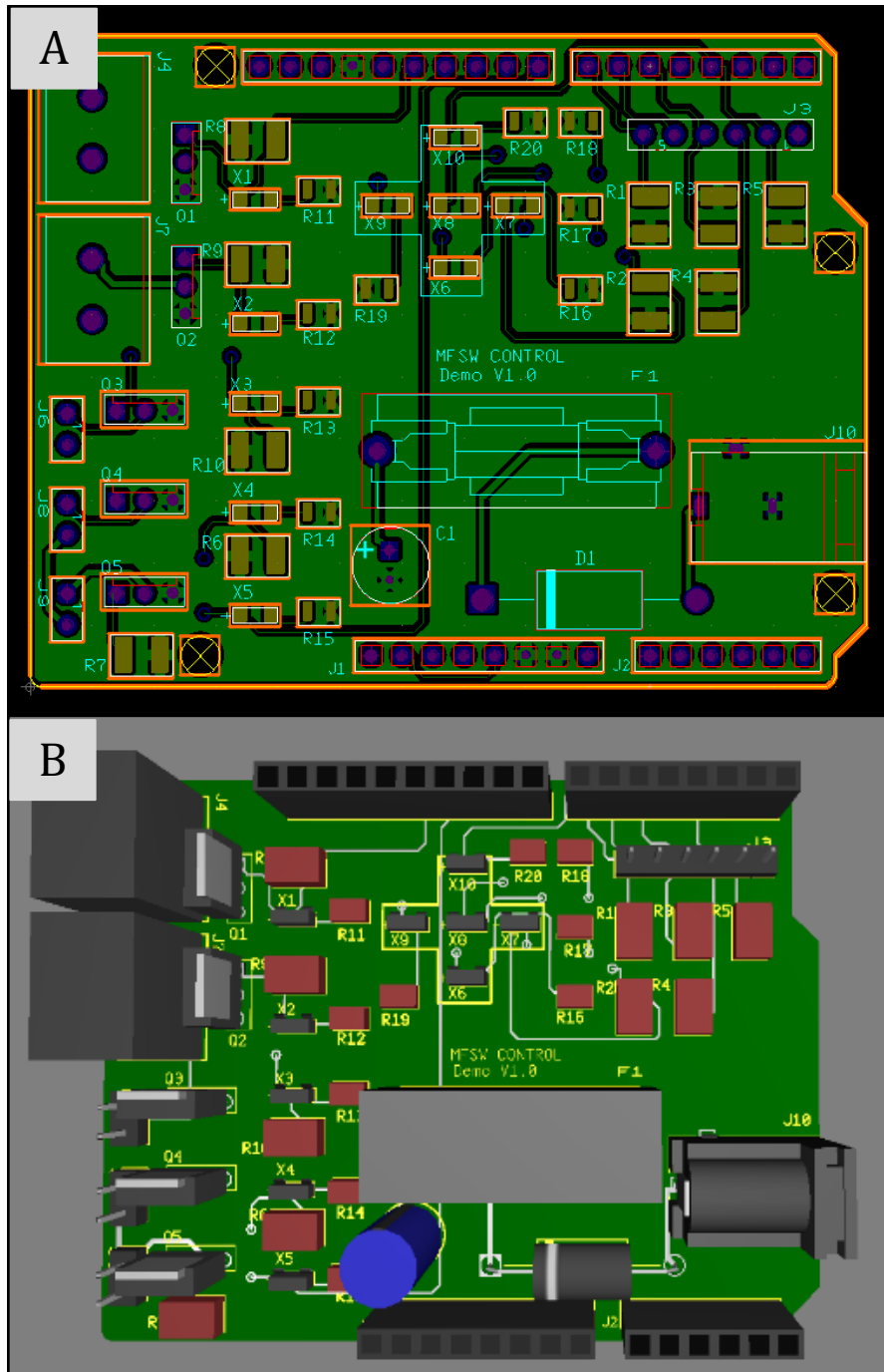
Figure 31 - 2D (A) and 3D (B) views of MFSD stand-alone control circuit

3.3 Device – Software

The Arduino™ IDE programming environment was used to develop logic for regulating the stand-alone control system for the MFSD. The IDE program contains convenient built-in software libraries of useful C-programming functions for microcontroller programming. The logic for the MFSD features a basic state-change machine architecture. Upon pressing each button (with exception of the middle button that controls illumination), the corresponding function activates momentarily (i.e. function is on for the duration of the button press). Upon pressing the button that controls illumination, LED brightness toggles from High-Medium-Low-Off in a circular fashion. Software is included in Appendix VI.

3.4 Verification & Validation

3.4.1 Benchtop Testing with Stand Alone Control

3.4.1.1 Leak Testing

Maintaining a leak-free environment in the AISS is vital considering the number of electronic components housed in the glovebox. For this reason, the suction/irrigation wand should be effectively leak-free when in a pressurized environment (e.g. the wound isolation domes). Given the textured surface of the metal wand finish, leak testing (setup in Figure 32) was performed by inserting the suction/irrigation wand into the wound isolation dome and visually inspecting for leaks at the wand/tubing interface. Pressures between 0 – 100 mmHg were evaluated.

Figure 32 – Benchtop leak test setup

3.4.1.2 Suction/Irrigation Flow Rate Testing

As indicated in the design objectives, endoscopic flow rates should reach

1 L/min. Flow rate testing (setup in Figure 33) was performed to verify that the

chosen peristaltic pumps were capable of reaching this threshold. The volumetric
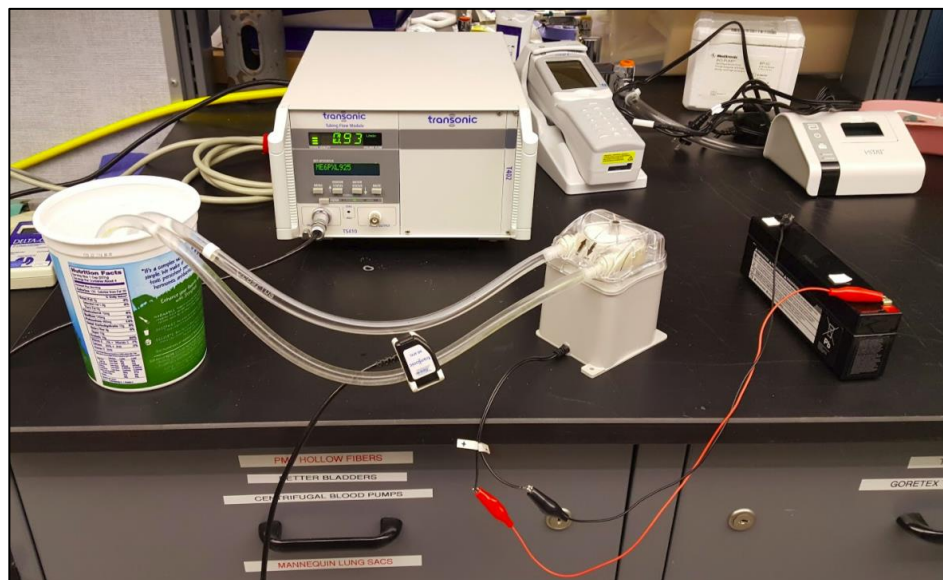
Figure 33 - Benchtop flow rate testing setup utilizing Transonic ME 6PXL flow probe

flow rate of the peristaltic pump was measured using a Transonic T410 Tubing

Flow Module with a Transonic ME 6PXL flow probe. A simple circuit was devised

connecting the pump to a reservoir with 1/4" PVC tubing. Prior to loading the DC

batteries, the voltage potentials (V) were measured using the Fluke 77

multimeter. DC voltage was then applied to the pump, and the settling flow rate

(L/min) after one minute was recorded.

3.4.1.3 Illumination Testing

The illumination function was also evaluated to assess the fiber optic's

ability to provide localized visualization. To perform this test, the fiber optic

illuminator (with epoxy potting to minimize light leakage) was connected to a

power source. The voltage potential of the power source was set to both 12 V

and 24 V. Illumination was assessed visually and quantified using Light Meter

(Version 2.0, Elena Polyanskaya), an iPhone application that measures

luminescence in terms of lux and foot-candles.

3.4.1.4 Stand-Alone Control Testing

After assembling the Arduino™ and control PCB, the stand-alone

controller was evaluated on the benchtop to confirm functionality. First, the logic

was uploaded onto the Arduino™ platform via USB connection to a PC. This

connection provided 5V power to the board, which allowed for confirmation of

each button press. As a specific function is activated on the button switch PCB,

the corresponding LED (inside the plus-sign region) on the control PCB should

illuminate. All five buttons were assessed to confirm the LEDS were functional (indicating a closed circuit) and correctly paired.

After confirming the button presses, the two peristaltic pumps, fiber optic LED, and indicator LEDs were connected to the control PCB. Additionally, a barrel power jack was inserted into the appropriate connector to supply 12 V power to the board and all hardware. This setup allowed for the confirmation of proper function activation following the corresponding button press. All three functions (suction, irrigation, illumination) and simulated functions (cut, coagulation) were assessed to verify the connections on the control PCB.

3.4.2 Intraoperative Testing

Intraoperative testing (setup in Figure 34) was performed in a porcine model to evaluate functionality in a surgical setting. Following the harvesting of the heart and the lungs for an unrelated study, the MFSD was tested *in vivo* to evaluate suction, irrigation, and illumination. Video recordings were taken during the activation of each function. Two iterations of this test were performed.
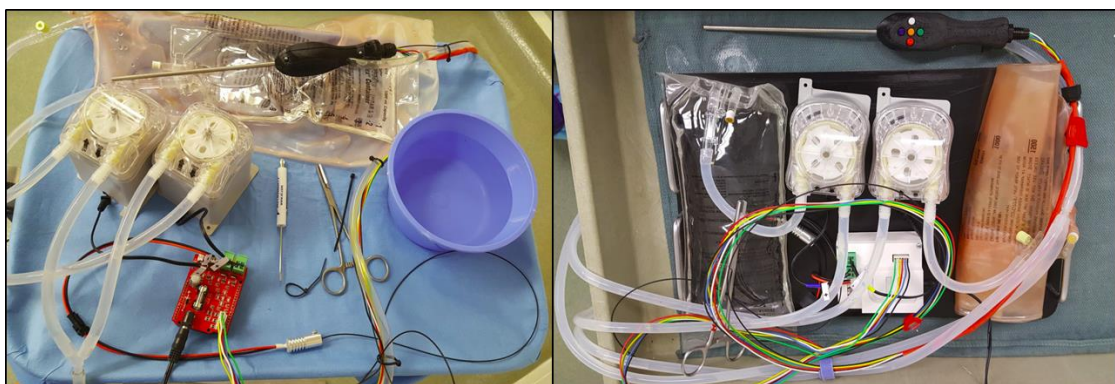
Figure 34 - Test setup for intraoperative animal testing

49

IV. RESULTS

4.1 Fabrication

4.1.1 Button Switch PCB

The button switch PCB (Figure 35) was fabricated using SeeedStudio. After receiving the PCB, the button switches and male header were soldered to the PCB as described in the methods. Upon pressing, each button provided a tactile and audible indication of actuation.
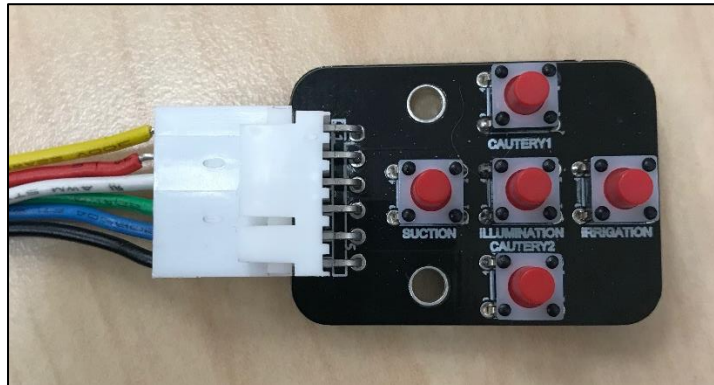
Figure 35 - Assembled button PCB

4.1.2 Silicone Button Pad

As shown in Figure 36, the resulting silicone part fit properly over the PCB assembly. The silicone mold was simple and low cost to fabricate; however, the resultant button pad was not as easy to activate as compared to the isolated button switches. The presence of the silicone material required the user to exert more force to actuate than the isolated button switch. In addition, the final part
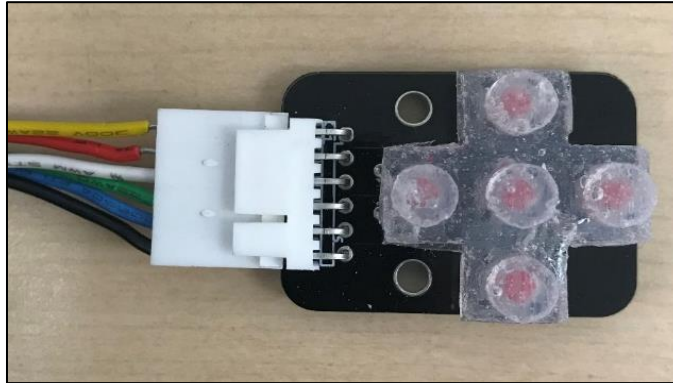
Figure 36 - Photograph of the silicone button pad on the button PCB

included small material imperfections (e.g., air bubbles) that formed during the

mold filling process, necessitating the need for an alternative design.

4.1.3 Pushbutton Caps

The five pushbutton caps were 3D printed as outlined in the methods. As

shown in Figure 37, the pushbutton caps fit securely over the button switches. In

comparison to the silicone pad, the plastic caps decreased the overall button

activation force. Further, the discrete nature of the pushbutton caps allowed for

more customization to provide chromatic and tactile button differentiation.
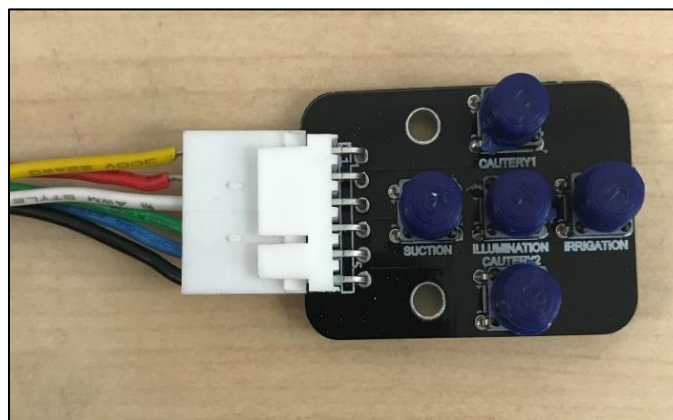
Figure 37 - Photograph of the plastic pushbutton caps on the button PCB

4.1.4 Fiber Optic Assembly

The fiber optic cable was adhered to the suction/irrigation wand and installed inside the opening in the fiber optic illuminator. Because this LED illuminator is manufactured for a 3 mm fiber optic cable (not 1.3 mm as chosen for this project), a small amount of opaque, blue putty was placed on the tip of the illuminator to prevent light leakage. Figure 38 illustrates this reduction in light leakage. Opaque potting epoxy (not pictured) was also used successfully to eliminate light leakage.
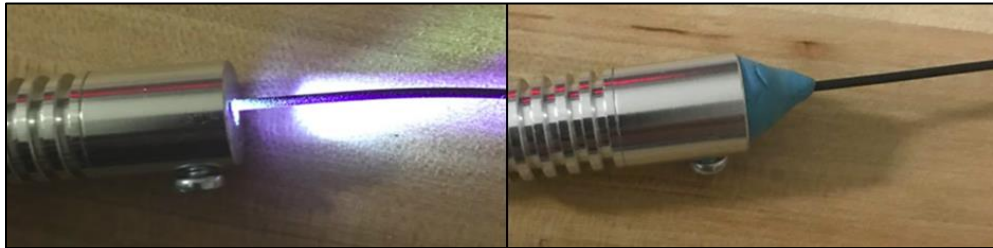
Figure 38 – Light leakage at fiber optic cable/illuminator interface (left); opaque putty placement that prevent light leakage at the fiber optic cable/illuminator interface (right)

4.1.5 Suction/Irrigation Wand

Despite the desirable material properties of Accura 60, the resultant product was too weak to withstand long-term usage (likely due to the thin part geometry). Figure 39 illustrates an example of a fracture that propagated after transport during device testing. Repairs were attempted using 3/16" heat-shrink tubing but were unsuccessful in restoring the component to its original condition. For these reasons, a metal version was fabricated.

Figure 39 - Fracture in Accura 60 suction/irrigation wand

The second suction/irrigation wand was created with 316L stainless steel.
The resultant part was significantly more durable that the plastic wand from the
previous manufacturing iteration. Figure 40 shows the distal tip of the stainless
steel SLS printed component. As 316L stainless steel is a harder material than
Accura 60, the finished product could not be sanded down to create a more
uniform surface finish. The rougher surface can also be seen in Figure 40.
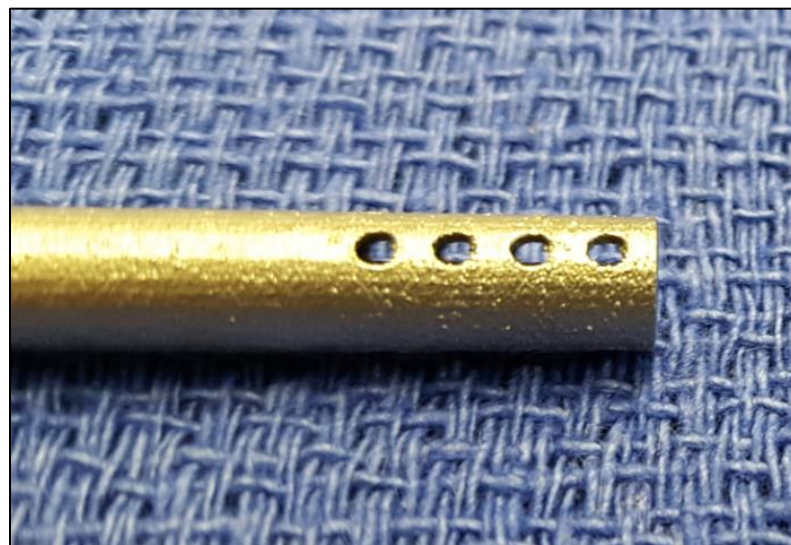
Figure 40 - Photograph of the distal tip of the stainless-steel suction/irrigation
wand

<u>4.1.6 Clamshell Handle</u>

In comparison to the proof-of-concept prototype, Prototype II featured a much more compact and sleek design. The overall length of the clamshell handle was decreased from 7.58 inches to 5.98 inches. In addition, the largest device width (in the front portion where the button switch PCB is housed) was minimized from 2.68 inches to 1.62 inches. As this prototype was completed during the earlier stages of device development, Prototype II featured the silicone button pad and plastic suction/irrigation wand (Figure 41). This prototype was a profound improvement from the proof-of-concept device in terms of ergonomics and assembly integrity.

Despite these advances, there were some features that called for additional design work. First, the newly shaped handle, while much more compact, was hard to stabilize when gripping with the index finger, middle finger, and thump due to its oblong, rounded shape. In addition, the suction/irrigation wand was placed too far inside of the clamshell handle. When inserting the distal shaft into the leak-free trocars, there was not enough device length to adequately manipulate the device inside the wound isolation dome.
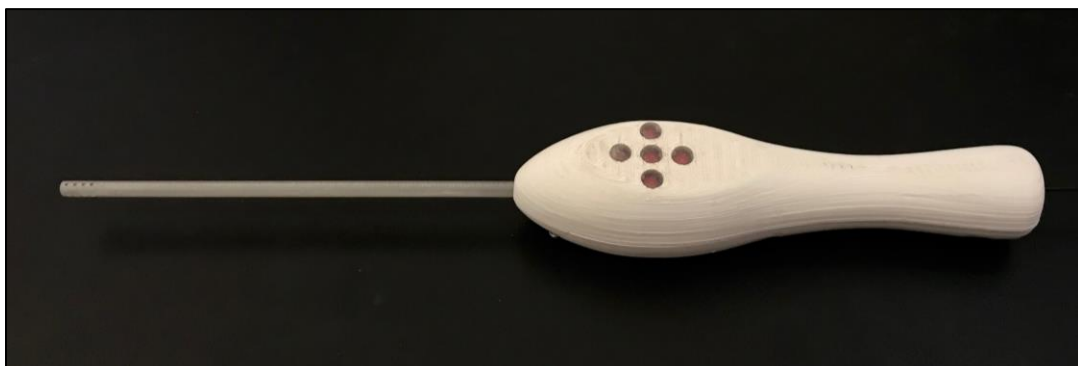
Figure 41 - Photograph of assembled Prototype II

Prototype III solved many of the issues discovered when evaluating

Prototype II. Figure 42 depicts Prototype III, which features flatter sides to

improve user handling and increased exposure length of the suction/irrigation

wand. Additionally, two of the small assembly screws with replaced with snap

fittings, in effort to reduce the effort required to assemble the device. This

prototype was much more comfortable for the user; however, the overall device

length was slightly too long, restricting easy installation into the suborbital

glovebox. In addition, the snap fittings added to the flat edge were too small and

easily broke upon assembling the device. Further, the seal created with snap

fittings was much less tight than the seal created with the small self-tapping

screws. For this reason, snap fittings were discontinued during this stage.
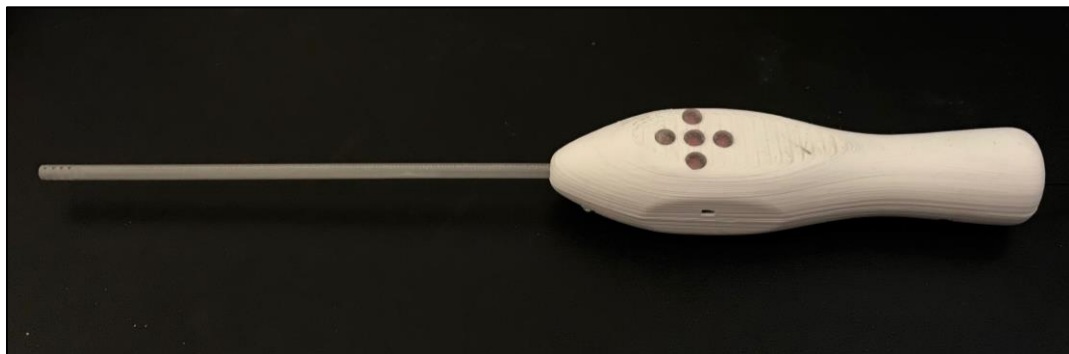
Figure 42 - Photograph of assembled Prototype III

Prototype IV (Figure 43) was the last device iteration that was fabricated

for this project. Because of material availability, this prototype was fabricated with

a black nGen filament (rather than white like earlier iterations). This final design

featured reductions in length of the clamshell handle (to 4.93 inches) and the

largest device width (to 1.3 inches).
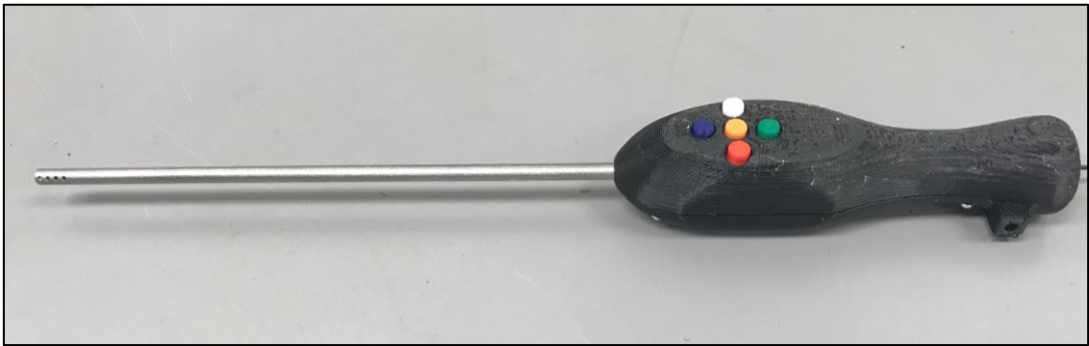
Figure 43 - Photograph of assembled Prototype IV

4.1.7 Stand-Alone Control PCB

Following the population of all electronic components, the control PCB

was mounted on top of the Arduino™ UNO as shown in Figure 44.
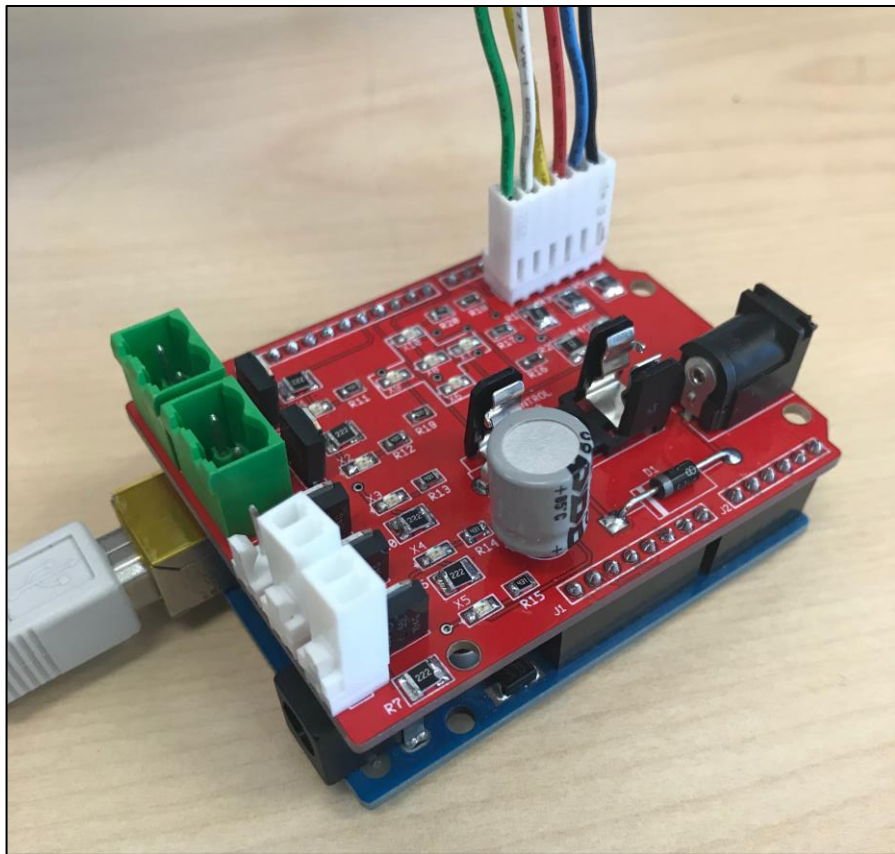
Figure 44 - Assembled MFSD stand-alone control circuit and Arduino™ UNO

4.1.8 Software

Appendix VI contains the complete code for the MFSD stand-alone control system. Figure 45 provides a graphical representation of the logic that was developed for the stand-alone controller. The setup portion initializes all variables and assigns input and output pins. The void loop runs through a sequence that checks for a button press and then momentarily activates the appropriate output until the button is no longer pressed.
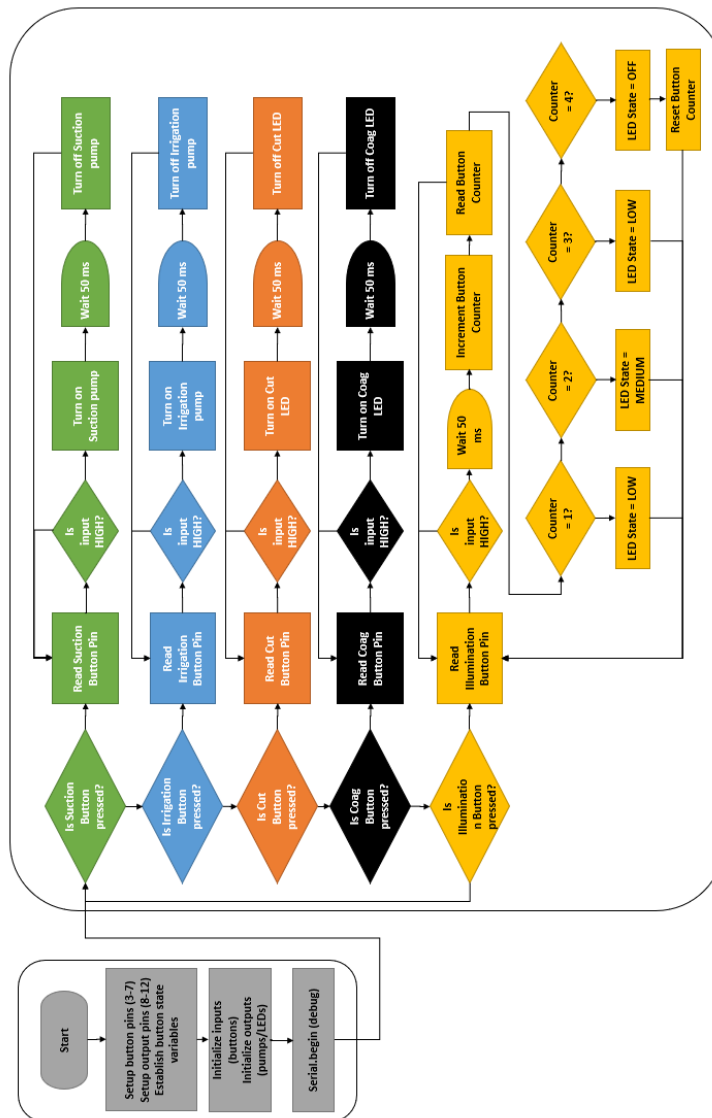
Figure 45 - Graphical representation of logic for stand-alone controller

4.2 Benchtop Testing

4.2.1 Leak Testing

When using the MFSD inside the pressurized environment of the dome, it is important that the seal created between the diaphragm of the trocar and the suction/irrigation wand is tight and leak-free. Leak testing was performed to verify this feature. After pressurizing the dome from 0 to 100 mmHg, the suction/irrigation wand was capable of preventing water leaks. Table 5 outlines the results from this test.

Table 5 - Results from suction/irrigation wand testing

Benchtop Leak Test	
UofL Suction/Irrigation Wand, 5mm trocar	
Simulator:	DeltaCal
Fluid Pressure (mm Hg)	Leakage Observed (Y/N)?
0	N
20	N
40	N
60	N
80	N
100	N
Pass/Fail:	PASS

4.2.2 Suction/Irrigation Flow Rate Testing

The peristaltic pumps were tested per the procedure outlined in the methods to evaluate suction and irrigation flow rate. Results indicated that an increase in measured voltage potential corresponded to an increase in settling flow rate for the peristaltic pump. At 12V, the pumps were capable of reaching the target flow rate (1 L/min) with a settling flow rate of 1.09 L/min.

Based on visual observation, the 24 V power supply provided brighter

localized illumination from the tip of the fiber optic cable; however, 12 V power

still provided adequate illumination. When measuring the luminescence output

using the Light Meter iPhone application, the 12 V and 24 V settings measured

260 lux and 300 lux, respectively. Based on these results, the illumination

function of the device will be powered by 24 V during the AISS suborbital test

flight. For benchtop testing purposes using the stand-alone control, however,

illumination will be powered by 12 V, as the electrical setup is much simpler for

testing the performance and configuration.

4.2.4 Stand-Alone Control Testing

Benchtop testing (Figure 46) with the control PCB was performed to

confirm: 1) correct pin assignment after each button press; and 2) correct

function activation after each button press. When connected to the 5V power
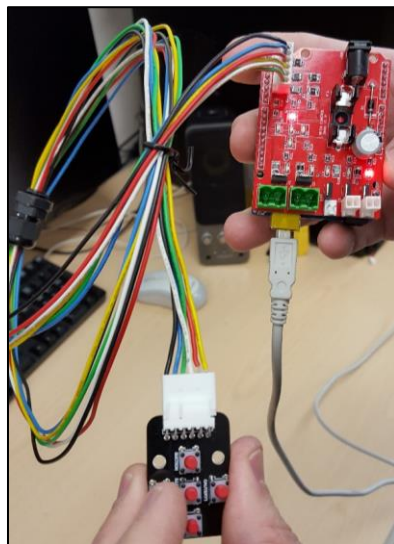
Figure 46 - Benchtop testing with control PCB to confirm correct LED
illumination upon button press (coagulation function is shown)

source to assess button/pin assignment, each button press correctly activated the corresponding indicator LEDs.

4.3 Intraoperative Testing

An intraoperative device test in a porcine model was the final performance test conducted before integrating with the FMS. After the heart and lung harvesting for the unrelated study was completed, the MFSD fluid line was primed to remove any trace of the air in the tubing. The device was handed to one of the animal testing surgeons who then demonstrated each function *in vivo.* During the first portion of the procedure, suction and irrigation were functioning correctly. Upon pressing and holding each button, each function initiated and worked at an adequate rate of flow. A photograph illustrating the suction function is shown in Figure 47 (note the blood in the fluid line existing the proximal tip of the wand). Irrigation functionality is also illustrated in Figure 48.

Figure 47 - Demonstration of suction functionality during intraoperative device testing
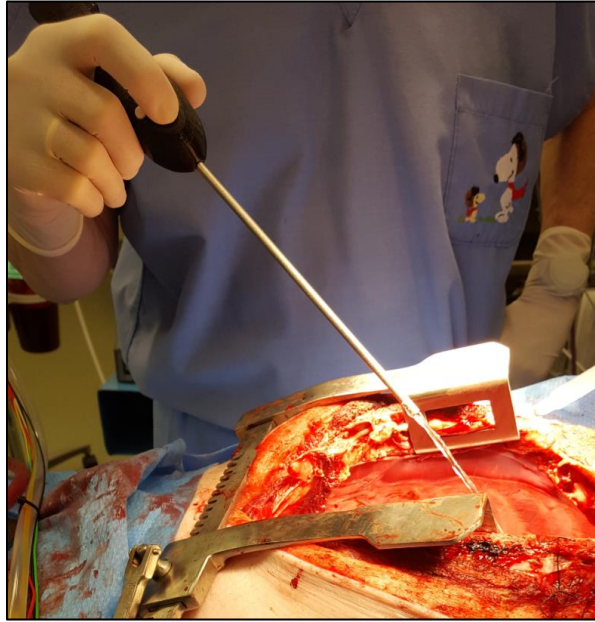
Figure 48 - Demonstration of irrigation functionality during intraoperative device testing

After the first few minutes of operating the device within the thoracic cavity of the animal, an electrical short (of unknown origin) took place on the control PCB. During the procedure, this became apparent when the button activation stopped working and the irrigation pump began to activate "spastically". While connected to power, the irrigation pump would activate briefly and repetitively without any user activation. This was the result of the electrical short on the PCB, which caused the Arduino ™ to reset every one second. At this point, the test procedure was stopped. The electrical issues were evaluated after properly cleaning the device and the fluid components to remove any traces of blood from the experiment. It was determined that a faulty connection in the wiring bundle connector and a missing grounding pad on the control PCB were to blame for the electrical malfunctions.

Following the correction of the electrical short, a second intraoperative test was conducted. This experiment was also performed in a porcine model following the removal of the heart and lungs. Unlike the first test, this demonstration of the MFSD was successful in demonstrating all three functions. The illumination function was first evaluated. After confirming that multiple button presses correctly toggled the brightness from Low-Medium-High-Off, the ability to locally illuminate was assessed. When inserting the distal tip of the wand into a poorly lit region of the thoracic cavity, the fiber optic adequately illuminated the site of interest. Because of the bright overhead lights in the operating room, the fiber optic did not enhance visualization in already well-lit areas. Figure 49 captures the brightest illumination of the fiber optic (left) and the localized illumination in a poorly lit area in the deep region of the thoracic cavity (right).
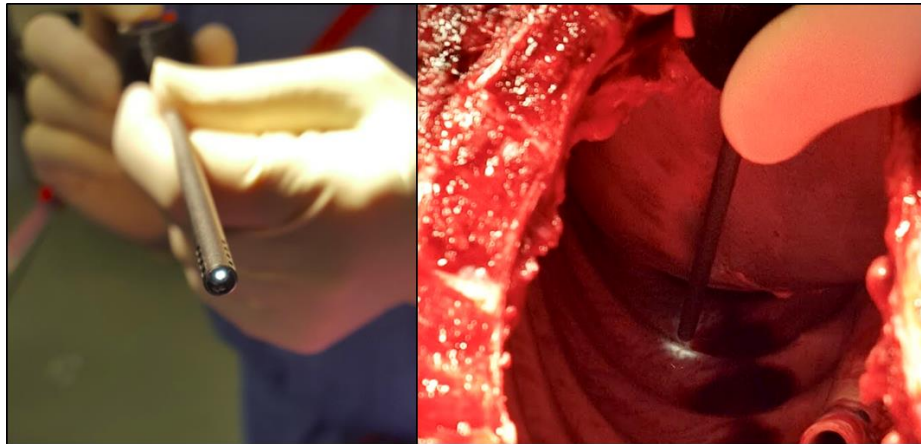
Figure 49 – Brightest illumination of fiber optic (left); localized illumination from fiber optic inside thoracic cavity (right)

Next the irrigation function was tested. Upon pressing the front blue button, irrigation initiated. The user demonstrated that the device was capable of enhancing visualization by irrigating to wash away blood for the site of interest. Suction testing yielded similar results. The function momentarily activated when

the user pressed the back green button. Additionally, suction helped restore visualization by removing blood that was obstructing the view. No electronic issues occurred during the activation of either function.

A final test intraoperative test was performed to assess the usability of the single fluid line. While the single channel for suction and irrigation is ideal from a design perspective (i.e. maintaining the desired circular geometry), the user must "clear the line" when switching from suction to irrigation. This means that the volume of blood that is in the fluid that has not passed the suction/irrigation split must exit the line and re-enter the operative field before the clean irrigation fluid can exit the device. Ideally, this intermittent volume should be minimized. To evaluate, suction was initiated until the line was full of blood and devoid of irrigation fluid (Figure 50). Then, irrigation was initiated and the line was cleared. Upon activating irrigation, there was roughly a four (4) second lag until clean irrigation fluid began flowing from the tip of the wand. At a 1 L/min flow rate, this time equates to roughly 67 mL of blood that must be cleared from the fluid line.
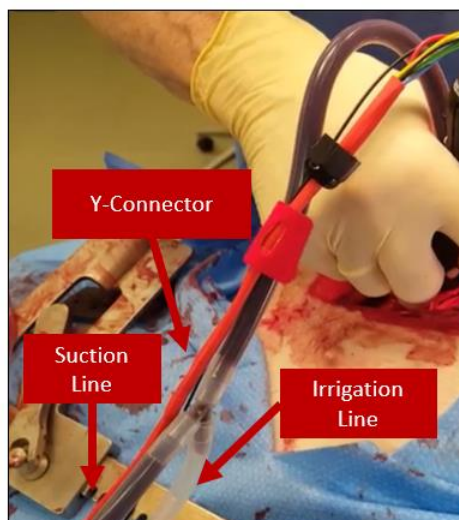
Figure 50 – Photograph of blood in the fluid line

V. DISCUSSION

5.1 Design Review

Based on results shown in Table 6, the final prototype of the MFSD met

and improved most design criteria in comparison to the proof-of-concept

prototype. Most significantly, adequate suction/irrigation flow rates were obtained

(1 L/min), the device was successfully instrumented to a stand-alone controller,

and the device handle was made much more comfortable and compatible for

Table 6 - Comparison of design objectives between proof of concept MFSD
(Prototype I) and final MFSD (Prototype IV)

	Rank	Prototype IV	Relative Score	Prototype I	Relative Score		
Customer Needs		**Device Comparison**				**Score**	**Rank**
Adequate suction/irrigation	5	4	9.76	2	4.88	1	Poor
Adequate illumination	5	3	7.32	1	2.44	2	Fair
Easy to assemble	3	4	9.76	3	7.32	3	Adequate
Can be instrumented to control circuit	5	5	12.20	2	4.88	4	Good
Ergonomic handle design	4	4	9.76	1	2.44	5	Excellent
Comfortable button-activation	3	4	9.76	4	9.76		
Low cost	1	2	4.88	2	4.88		
Lightweight	2	4	9.76	2	4.88		
Reliability	4	4	9.76	4	9.76		
Reusable	4	3	7.32	3	7.32		
Leak-free/water proof	5	4	9.76	3	7.32		
Total		**41**		**27**			

index-finger activation. In addition, illumination functionality was substantially improved and the MFSD was made much more lightweight by decreasing overall width and length. Appendix III provides dimensioned drawings for the fabricated MFSD components (top and bottom clamshells, suction/irrigation wand, pushbutton caps). Further, Appendix IV includes dimensioned drawings of both the exploded and collapsed configurations of Prototype IV.

Compared to Prototypes I, II, and II, Prototype IV was the most ergonomically designed, most compact, and most compatible with the AISS glovebox, shown in Figure 51. Table 7 outlines the major dimensions changed during each design iteration, demonstrating the progressive reduction in device size. In comparison to the proof of concept prototype, Prototype IV decreased overall device length by 6.66 inches, handle length by 2.65 inches, and largest device diameter by 1.38 inches.
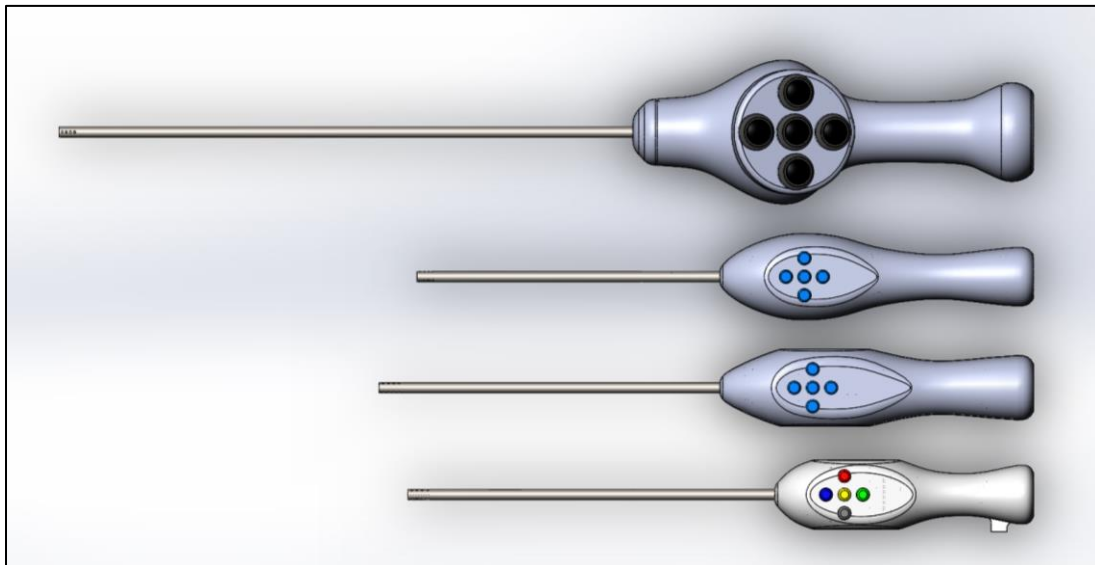
Figure 51 - Solid model illustrating the design progression of the MFSD assembly

Table 7 - Major dimension changes from Prototype I to Prototype IV

Component	Measurement	Design I	Design II	Design III	Design IV
Multifunctional device	Overall length	18.5 in	11.7 in	12.7 in	11.84 in
3D Printed Handle	Overall length	7.58 in	5.93 in	5.93 in	4.93 in
3D Printed Handle	Largest width	2.68 in	1.62 in	1.45 in	1.3 in
3D Printed Handle	Clamshell assembly	#4-40	#2, 0.5 "	Snap fittings, #2, 0.5"	#2, 0.5 "
3D Printed Handle	Handle diameter	1.12 in	0.84 in	1.0 in	0.79 in
Suction/irrigation wand	Length	15.75 in	10.5 in	10.5 in	10.5 in
Pushbutton	Largest diameter	0.69 in	0.28 in	0.28 in	0.28 in
Fiber optic cable	Major diameter	1.0 mm	1.3 mm	1.3 mm	1.3 mm

5.2 Limitations

Despite the design progress of Prototype IV, there are some inherent limitations due to time and monetary constraints of the project. First is the fabrication of the device. Measures were taken to help eliminate the potential for water-leakage; however, the clamshell handles are not fully water-proof. It is possible for water to enter the device via the small spaces around the pushbutton caps, the lip between the clamshell halves, or the openings for the cable gland and the silicone tubing. Future modifications in material choice and assembly methods could eliminate this risk.

A second limitation is the lack of mechanical testing. Mechanical loading is an important aspect of device testing during the FDA regulatory approval process. More testing of the device would be required to determine whether the

device is suitable for surgical use. For instance, common mechanical tests include failure testing of components to ensure durability and activation force testing to ensure ergonomic compatibility with surgeons.

Another limitation is the ease of sterilization. With increased multifunctionality, device designs become less simplistic. As devices become more complex, difficulties will arise with device assembly and sterilization [28].

Finally, a small test sample size (n=2 porcine experiments) of the intraoperative test was performed to demonstrate device performance *in vivo*. Larger sample size based upon a power analysis will be required to determine statistical significance of the device functionality during future testing (both *in vivo* and benchtop). In addition, no testing has been performed in an endoscopic surgical setting.

<center>5.3 Future Work</center>

5.3.1 FMS Integration

There are several opportunities to further the development of the MFSD and related surgical capabilities for exploration space missions. Most immediate is the integration of the MFSD with the AISS Fluid Management System that is currently in development. Once the AISS is fully-automated, the technology will fly and be evaluated on a suborbital mission before the end of 2018. The flight on Virgin Galactic's SpaceShipTwo (Figure 52) will reach a peak altitude of 65 miles and provide approximately 3 minutes of high-quality microgravity for the evaluation of the integrated subsystems.

<center>67</center>

During this flight, the MFSD will be tested for three functions; 1) the ability to suction a small injection of analog blood (i.e. glycerin, water, and food coloring) from the saline-pressurized dome; 2) the ability to irrigate saline onto a simulated bleeding wound site to restore visualization; and 3) the ability to locally illuminate the surgical site of interest to provide enhanced illumination. High-definition surveillance cameras mounted inside the payload will record experiment status throughout the entire flight from takeoff to landing. Figure 53 provides a graphical representation of the FMS and MFSD integrated fluid functions for the suborbital flight test. Additional testing on parabolic flights for further AISS surgeon-system integrated testing is anticipated.
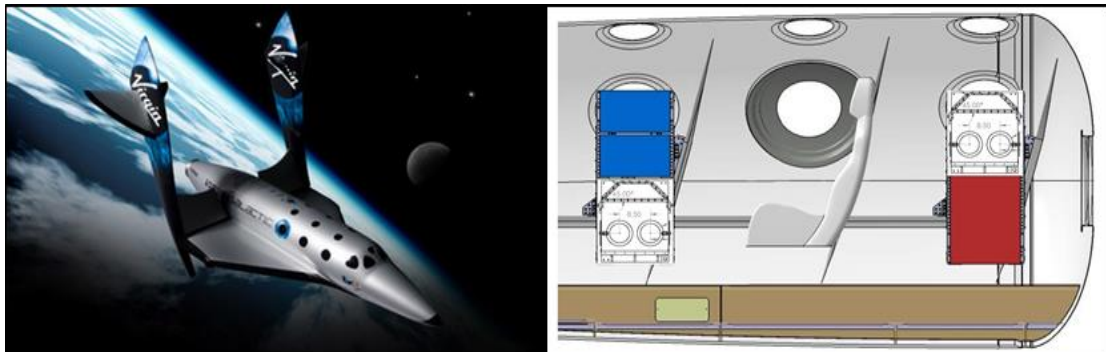
Figure 52 - Virgin Galactic's SpaceShipTwo (left); possible glovebox positions in the cabin of SpaceShipTwo (right)

5.3.2. Additional Features

Future development of the MFSD includes the integration of cautery (with both cut and coagulation settings) and visualization. Cautery will most likely be provided by a pair of bipolar electrodes, while visualization will be provided by a small fiber optic cable. The addition of these two functions will necessitate the development of a more complex suction/irrigation wand that provides additional channels for these functions.

Additional features could be integrated into the wand to support surgical tasks. For example, smoke suction is an important device function for ground procedures, considering surgeon's periodic inhalation of smoke generated from electrocautery devices. Grasping and retracting functions could also be implemented to assist with surgical manipulation of organs and surrounding tissues.
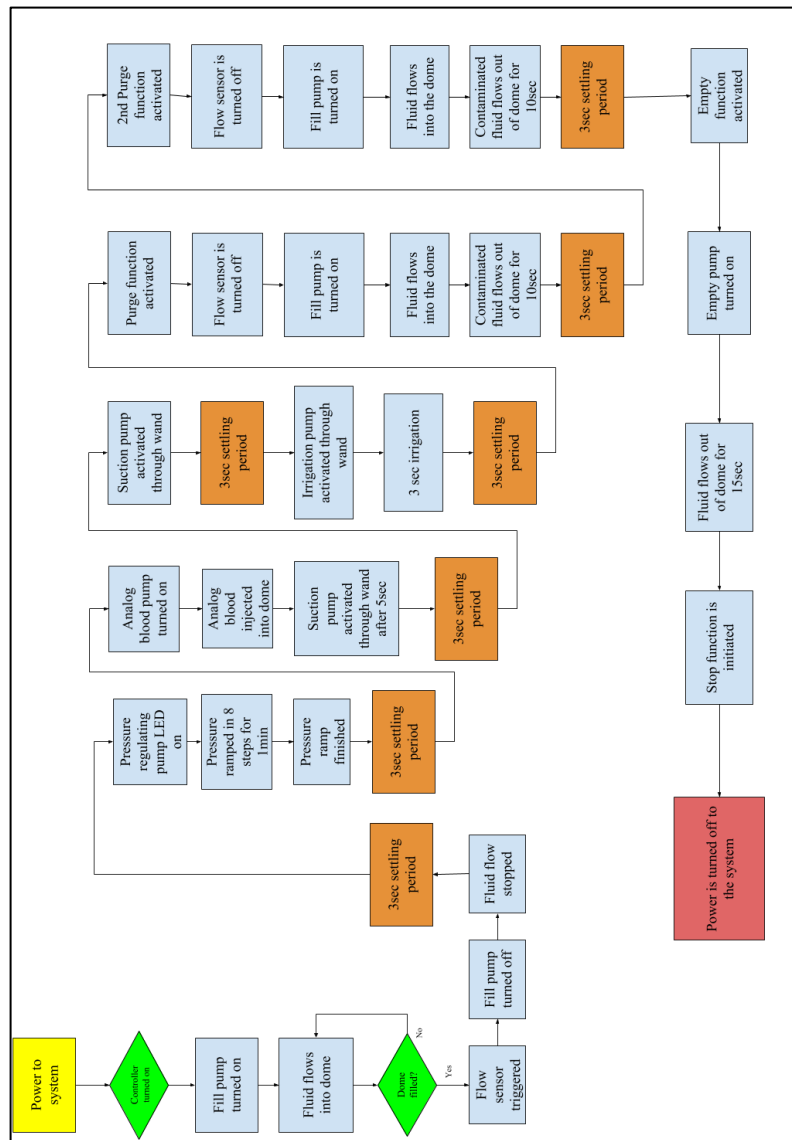
Figure 53 – Test sequence for fully-automated suborbital flight test

VI. CONCLUSION

The primary objective of this M.Eng. thesis was to design and develop a multifunctional surgical device that integrates suction, irrigation, and illumination functionality into a single device. Preliminary benchtop and intraoperative porcine testing has demonstrated feasibility as evidenced by adequate suction/irrigation flow rates and enhanced, localized illumination. Future development work will focus on: 1) integration with the AISS Fluid Management System for fully-automated system suborbital flight testing later in 2018; and 2) the incorporation of cautery – both cut and coagulation—and visualization functionality to the device. Further development and additional benchtop and microgravity testing of this technology will result in a fully-functional MFSD to provide astronauts with the necessary surgical capabilities during projected exploration space missions.

In addition to space exploration missions, other applications for the MFSD include both open and endoscopic (e.g. laparoscopy and arthroscopy) surgical procedures. The MFSD enables the user to activate multiple surgical functions using a single instrument, reducing the number of instrument exchanges during a procedure, thus reducing time and cost to patients and insurers. The reduction instrument exchange can also help maintain surgeon focus, potentially contributing to better patient outcomes.

VII. LIST OF REFERENCES

1. Hayden, J.A., et al., *A hermetically sealed, fluid-filled surgical enclosure for microgravity.* Aviat Space Environ Med, 2013. **84**(12): p. 1298-303.
2. Nicogossian, A. and D. Pober, *The future of space medicine.* Acta Astronaut, 2001. **49**(3-10): p. 529-35.
3. G., C., *Fundamentals of space medicine. .* Norwell, MA: Springer and Microcosm Press, 2005.
4. Campbell, M.R. and R.D. Billica, *A review of microgravity surgical investigations.* Aviat Space Environ Med, 1992. **63**(6): p. 524-8.
5. Hurlbert K, B.B., Carroll C, Jeevaranjan A, Kliss M, Singh B. , *Draft human health, life support, and habitation systems - technology area 06. .* Washington DC: National Aeronautics and Space Administration, 2010.
6. NASA. *NASA: About.* 2018 [cited 2018 March 18]; Available from: https://www.nasa.gov/about/index.html.
7. Baisden, D.L., et al., *Human health and performance for long-duration spaceflight.* Aviat Space Environ Med, 2008. **79**(6): p. 629-35.
8. Nicogossian, A., *Medicine and space exploration.* Lancet, 2003. **362 Suppl**: p. s8-9.
9. Rafiq, A., et al., *Microgravity effects on fine motor skills: tying surgical knots during parabolic flight.* Aviat Space Environ Med, 2006. **77**(8): p. 852-6.
10. Haidegger, T., J. Sandor, and Z. Benyo, *Surgery in space: the future of robotic telesurgery.* Surg Endosc, 2011. **25**(3): p. 681-90.
11. Allen CS, B.R., Charles J, Cucinotta F, Fullerton R, Goodman JR, Griffith AD, Kosmo JJ, Perchonok M, Railsback J, Rajulu S, Stilwell D, Thomas G, Tri T, *Guidelines and capabilities for designing human missions.* NASA/Johnson Space Center, 2003. **TM-2003-210785**.
12. Campbell, M.R., et al., *Endoscopic surgery in weightlessness: the investigation of basic principles for surgery in space.* Surg Endosc, 2001. **15**(12): p. 1413-8.
13. Bogomolov, V.V., et al., *International Space Station medical standards and certification for space flight participants.* Aviat Space Environ Med, 2007. **78**(12): p. 1162-9.
14. Davis, J.R., *Medical issues for a mission to Mars.* Aviat Space Environ Med, 1978. **70**: p. 162-168.
15. Barratt, M., *Medical support for the international space station.* Aviat Space Environ Med, 1998. **70**: p. 155-161.
16. Jennings, R.T., et al., *Medical qualification of a commercial spaceflight participant: not your average astronaut.* Aviat Space Environ Med, 2006. **77**(5): p. 475-84.
17. Pease, R.e., *Medical dictionary. .* Merriam-Webster, USA, 2003.
18. Scientist, N. *Doctors remove tumor in first zero-g surgery.* New Scientist 2006.
19. Kirkpatrick, A.W.B., CG. Campbell, M. Williams, DR. Parazynski, SE. et al. , *Severe traumatic injury during long duration spaceflight: Lights years beyond ATLS. .* J Trauma Manag Outcomes, 2009. **3**(4).

20. Campbell, M.R., *A review of surgical care in space.* J Am Coll Surg, 2002. **194**(6): p. 802-12.

21. Campbell, M.R., R.D. Billica, and S.L. Johnston, 3rd, *Animal surgery in microgravity.* Aviat Space Environ Med, 1993. **64**(1): p. 58-62.

22. Montidoro, T.A., J.E. Burgess, and J.F. Antaki, *Characterizing Pressure and Flow Rate for Aqueous Immersion Surgery.* Surg Innov, 2016. **23**(1): p. 36-41.

23. McCuaig, K., *Aseptic technique in microgravity.* Surg Gynecol Obstet, 1992. **175**(5): p. 466-76.

24. Matern, U., *Ergonomic deficiencies in the operating room: examples from minimally invasive surgery.* Work, 2009. **33**(2): p. 165-8.

25. Amaral, J.F., *Laparoscopic cholecystectomy in 200 consecutive patients using an ultrasonically activated scalpel.* Surg Laparosc Endosc, 1995. **5**(4): p. 255-62.

26. Geis, W.P., et al., *Synergistic benefits of combined technologies in complex, minimally invasive surgical procedures. Clinical experience and educational processes.* Surg Endosc, 1996. **10**(10): p. 1025-8.

27. Mehta, N.Y., et al., *Sequence and task analysis of instrument use in common laparoscopic procedures.* Surg Endosc, 2002. **16**(2): p. 280-5.

28. Frecker, M.I., et al., *Laparoscopic multifunctional instruments: design and testing of initial prototypes.* JSLS, 2005. **9**(1): p. 105-12.

29. Claus, G.P., et al., *Quantitative standardised analysis of advanced laparoscopic surgical procedures.* Endosc Surg Allied Technol, 1995. **3**(4): p. 210-3.

30. Melzer, A., *Endoscopic instruments: conventional and intelligent. .* Endosurgery, 1996: p. 69-95.

31. den Boer, K.T., et al., *Quantitative analysis of the functionality and efficiency of three surgical dissection techniques: a time-motion analysis.* J Laparoendosc Adv Surg Tech A, 1999. **9**(5): p. 389-95.

32. Sjoerdsma, W., et al., *Comparison of efficiencies of three techniques for colon surgery.* J Laparoendosc Adv Surg Tech A, 2000. **10**(1): p. 47-53.

33. Honlite Industrial Co., L. *1000 mL/min, 12V Peristaltic Pump with Exchangeable Pump Head.* 2018 [cited 2018 April 21]; Available from: https://honlitepump.en.alibaba.com/product/60379704032-802504748/1000ml_mim_24V_Peristaltic_Pump_with_Exchangeable_Pump_Head_and_FDA_approved_PharMed_BPT_Peristaltic_Tube_.html.

34. Seeed Technology Co., L. *Seeed Studio Fusion.* 2018; Available from: https://www.seeedstudio.com/fusion.html.

35. Protolabs. *How 3D Printing Materials Measure Up.* 2018 March 13]; Available from: https://www.protolabs.com/media/1010900/stainlesssteel-316l-material-spec-data-sheet-02.pdf.

36. Protolabs. *Stainless Steel 316 L Material Specifications.* 2018 [cited 2018 March 13]; Available from: https://www.protolabs.com/resources/design-tips/3d-printing-materials/.

37. *nGen.* 2018 [cited 2018 April 15]; Available from: https://colorfabb.com/materials/co-polyesters/ngen.

38. Arduino. *Arduino Uno Rev3.* 2018 [cited 2018 March 13]; Available from: https://store.arduino.cc/usa/arduino-uno-rev3.

VIII. APPENDIX I: CONTROL PCB SCHEMATIC
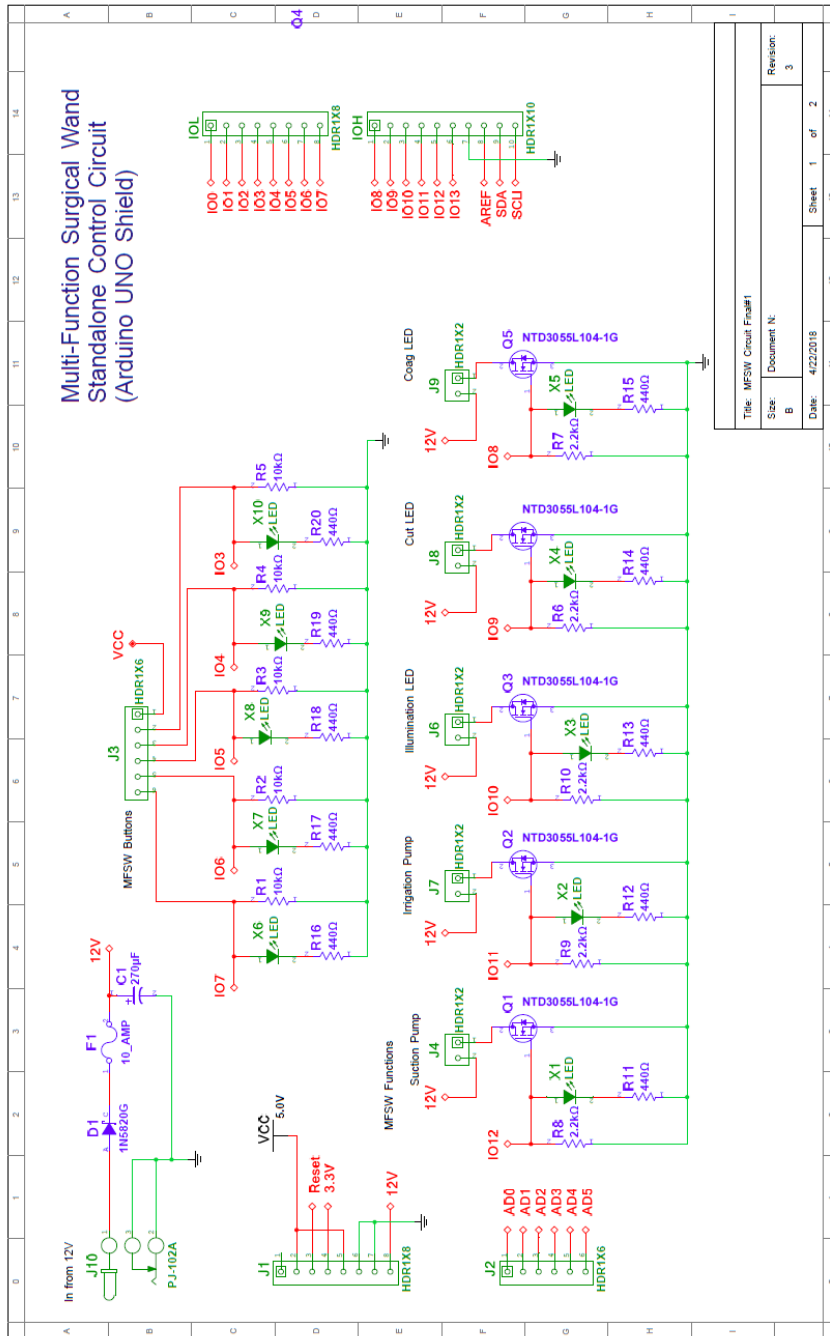
IX. APPENDIX II: BILL OF MATERIALS

VALUE	QUANTITY	REFERENCE	FOOTPRINT
HDR1X6	1	J1	HDR1X6HA
SPST	5	CAUTERY1, CAUTERY2, ILLUMINATION, IRRIGATION, SUCTION	THT BUTTON

Button Switch PCB – Bill of Materials

VALUE	QUANTITY	REFERENCE	FOOTPRINT
1N5820G	1	D1	DIOAD1760W125L840D505P
2.2kOhm	5	R6,R7,R8,R9,R10	R1210
10_AMP	1	F1	FUSE20X5R23
10kOhm	5	R1,R2,R3,R4,R5	R1210
270uF	1	C1	CAPPR250-630X1120
440Ohm	10	R11,R12,R13,R14,R15,R16,R17,R18,R19,R20	R0805
HDR1X2	2	J4,J7	2pin vertical
HDR1X2	3	J6,J8,J9	HDR1X2
HDR1X6	1	J2	Arduino_HDR1X6
HDR1X6	1	J3	HDR1X6
HDR1X8	2	IOL,J1	Arduino_HDR1X8
HDR1X10	1	IOH	Arduino_HDR1X10
LED	10	X1,X2,X3,X4,X5,X6,X7,X8,X9,X10	LED 0805(2012) w RefDes
NTD3055L104-1G	5	Q1,Q2,Q3,Q4,Q5	TO229P239X654X978-3P
PJ-102A	1	J10	CUI_PJ-102A

Stand-Alone Control PCB – Bill of Materials

X. APPENDIX III: DRAWINGS OF MFSD COMPONENT

Brooke Barrow

TITLE: Clamshell Top 4

R0.10

R0.14

SIZE **A** DWG. NO. CLAMSHELL TOP 4

REV

SCALE: 1:2

SHEET 1 OF 1

Ø0.82

Ø0.08 x4

R0.13 x5

Ø0.20

1.54

1.72

0.13

0.05

4.90

2°

DO NOT SCALE DRAWING

R0.55
R0.41

Brooke Barrow

TITLE:
Clamshell Bottom 4

SIZE | DWG. NO. REV
A | CLAMSHELL BOTTOM 4

SCALE: 1:2   SHEET 1 OF 1

1.30
Ø 0.50
1.51
Ø 0.20

0.13
0.05
0.51
2.21
0.60
4.90

DO NOT SCALE DRAWING

B

A

1

2

DETAIL A
SCALE 3 : 1

Ø0.07

R0.15

R0.08

9.64

0.17

0.16

1.04

0.05

Ø0.30

1.04

A

A

B

B

1

1

2

2

Brooke Barrow

TITLE:

Suction/Irrigation Wand

SIZE | DWG. NO. | REV
A | SUCTION IRRIGATION WAND |

SCALE: 1:5 | SHEET 1 OF 1

DO NOT SCALE DRAWING

77

0.24

0.18

0.06

R0.04

Ø0.16

Ø0.24

Ø0.28

Brooke Barrow

TITLE:
Single Pushbutton Cap

DWG. NO.
SINGLE PUSHBUTTON CAP

REV

SIZE
A

SCALE: 5:1

SHEET 1 OF 1

XI. APPENDIX IV: DRAWINGS OF MFSD ASSEMBLY

R0.55

R0.41

Brooke Barrow

TITLE:

MFSD Assembly

SIZE DWG. NO.   REV
A   PROTOTYPE IV ASSEMBLY

SCALE: 1:5   SHEET 1 OF 1

Ø0.82

0.30

1.54

4.90

11.84

8.55

6.95

1.30

0.15

DO NOT SCALE DRAWING
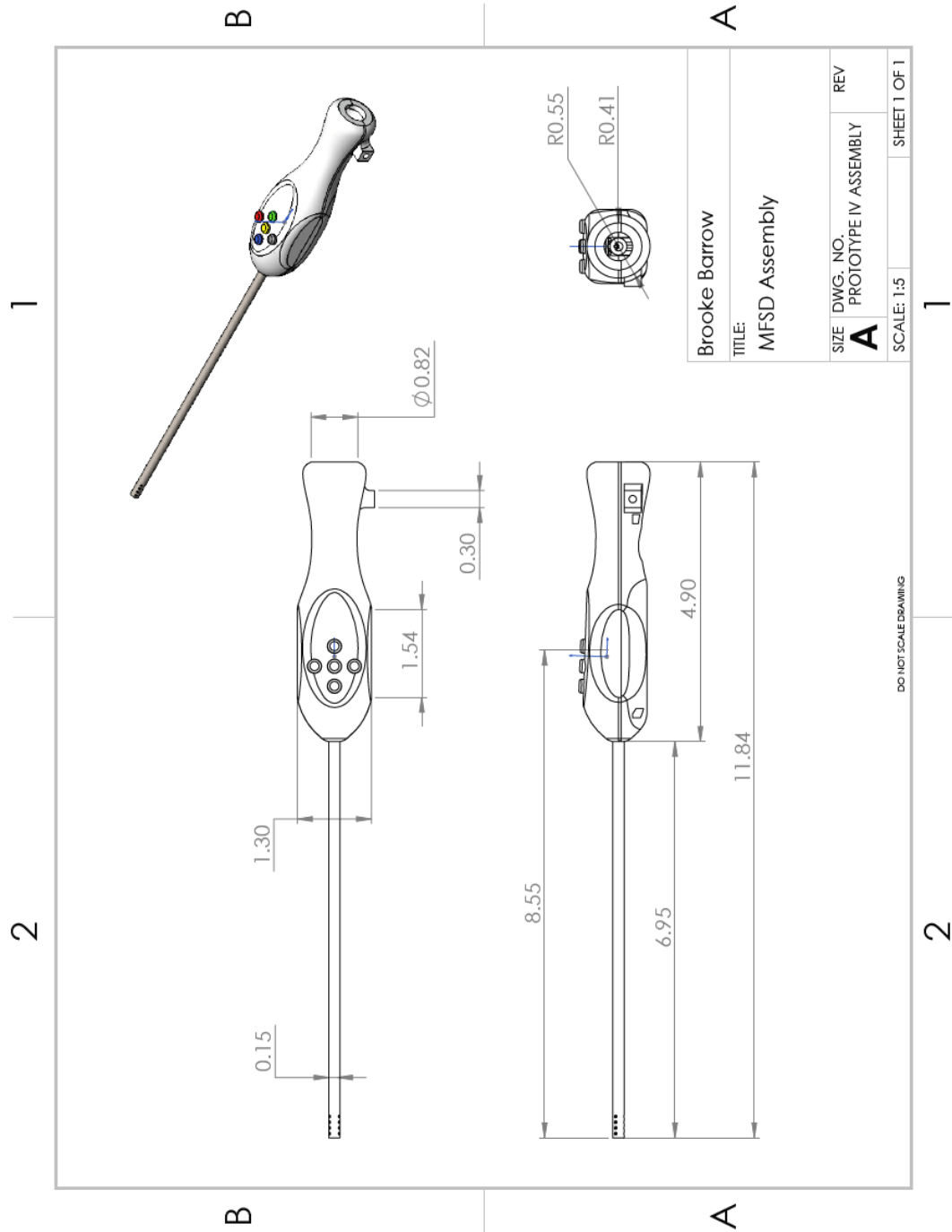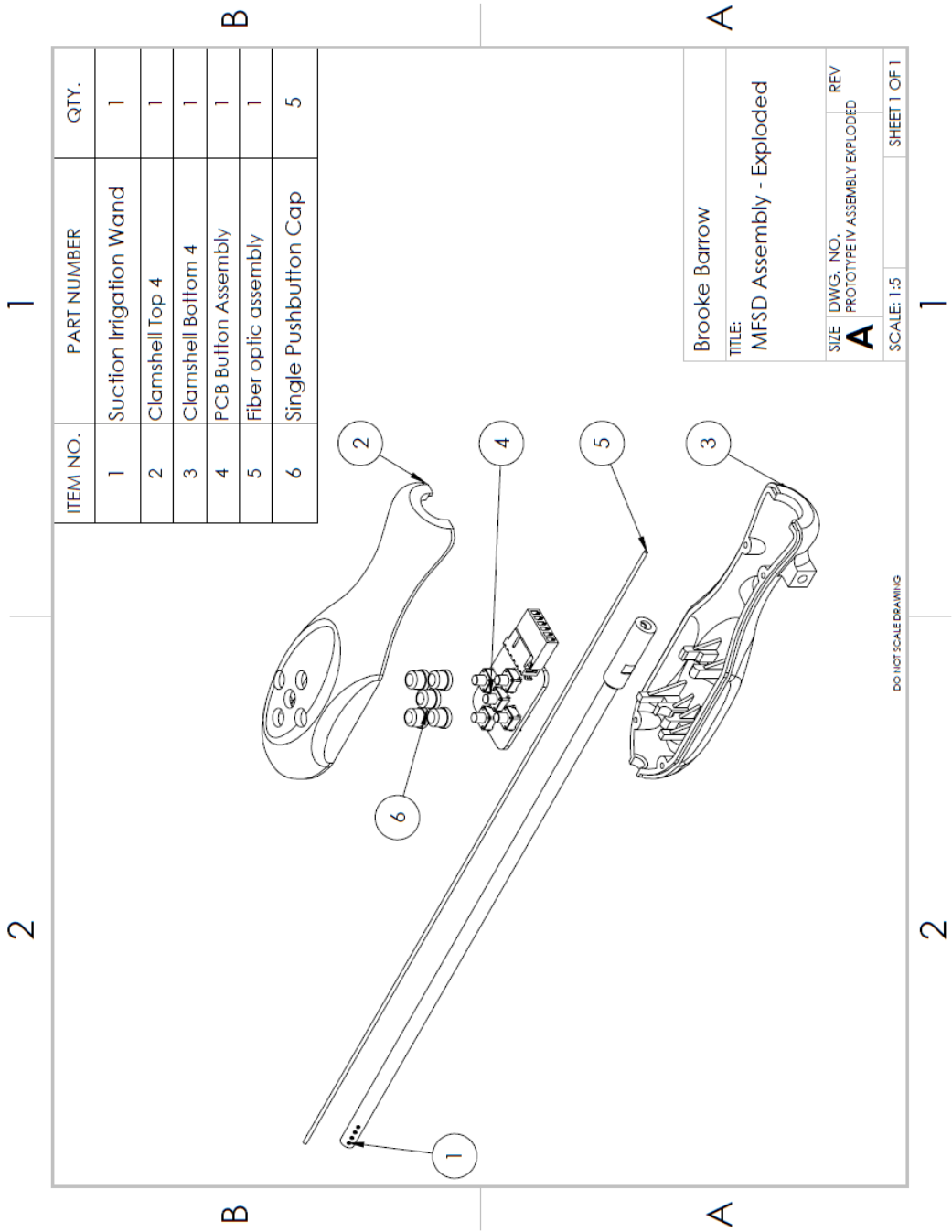
ITEM NO.	PART NUMBER	QTY.
1	Suction Irrigation Wand	1
2	Clamshell Top 4	1
3	Clamshell Bottom 4	1
4	PCB Button Assembly	1
5	Fiber optic assembly	1
6	Single Pushbutton Cap	5

Brooke Barrow

TITLE:

MFSD Assembly - Exploded

SIZE **A** | DWG. NO. | REV
PROTOTYPE IV ASSEMBLY EXPLODED

SCALE: 1:5 | SHEET 1 OF 1

DO NOT SCALE DRAWING

XII. APPENDIX V: 3D PRINTER SETTINGS

Printer Details	
Filament Type	ColorFabb nGen 3.00 mm
Printer	Lulzbot Taz 6
Bed Adhesion	Hairspray/IPA
Settings	
Layer Height (mm)	0.2
Shell Thickness (mm)	1
Enable Retraction	Checked
Bottom/Top Thickness (mm)	1.14
Fill Density (%)	15
Perimeters before Infill	Checked
Print speed (mm/s)	50
Printing Temperature (*C)	230
Bed temperature (*C)	85
Support Type	Everywhere
Platform Adhesion Type	None
Diameter (mm)	2.89
Flow (%)	100
Nozzle size (mm)	0.5
Speed (mm/s)	10
Distance (mm)	1
Initial Layer thickness (mm)	0
Initial layer line width (%)	125
Cut off object bottom (mm)	0
Dual extrusion overlap (mm)	0.15
Travel speed (mm/s)	175
Bottom layer speed (mm/s)	8
Infill speed (mm/s)	30
Top/bottom speed (mm/s)	20
Outer shell speed (mm/s)	20
Inner shell speed (mm/s)	25
Minimal layer time (sec)	10
Enable cooling fan	Checked

XIII. APPENDIX VI: MFSD SYSTEM CODE FOR ARDUINO/CONTROL PCB

```
/*  Manual code for MFSD */

// assign pins for pushbutton inputs
const int suctionButtonPin = 7;
const int irrigationButtonPin = 3;
const int illuminationButtonPin = 5;
const int cutButtonPin = 6;
const int coagButtonPin = 4;

// assign pins for outputs
const int suctionPump = 12;              // output to GATE of MOSFET for pump 1
const int irrigationPump = 11;           // output to GATE of MOSFET for pump 2
const int illuminationLED = 10;          // output to GATE of MOSFET for LED
const int cutLED = 8;                    // output to LED indicator placeholder 1
const int coagLED = 9;                   // output to LED indicator placeholder 2

// variables
int suctionButtonState = 0;              // current suction button state
int irrigationButtonState = 0;           // current irrigation button state
int cutButtonState = 0;                  // current cut button state
int coagButtonState = 0;                 // current coag button state

int LEDbuttonState = 0;                  // current illumination button state
int LEDbuttonPushCounter = 0;            // counts button presses for illumination
int LEDlastButtonState = 0;              // previous illumination button state

void setup() {
  // initialize buttons as inputs
  pinMode(suctionButtonPin, INPUT);
  pinMode(irrigationButtonPin, INPUT);
  pinMode(illuminationButtonPin, INPUT);
  pinMode(cutButtonPin, INPUT);
  pinMode(coagButtonPin, INPUT);

  // initialize connection to GATEs of MOSFETs as outputs
  pinMode(suctionPump, OUTPUT);
```

```
  pinMode(irrigationPump, OUTPUT);
  pinMode(illuminationLED, OUTPUT);
  pinMode(cutLED, OUTPUT);
  pinMode(coagLED, OUTPUT);

  //Debug
  Serial.begin(9600);
}

void loop() {
  // read pushbutton pins
  suctionButtonState = digitalRead(suctionButtonPin);
  irrigationButtonState = digitalRead(irrigationButtonPin);
  LEDbuttonState = digitalRead(illuminationButtonPin);
  cutButtonState = digitalRead(cutButtonPin);
  coagButtonState = digitalRead(coagButtonPin);

  // compare Illumination state to previous state
  if (LEDbuttonState != LEDlastButtonState) {
    LEDbuttonPressed();
  }
  if (suctionButtonState == HIGH){
    suctionButtonPressed();
  }
  else if (irrigationButtonState == HIGH) {
    irrigationButtonPressed();
  }
  else if (cutButtonState == HIGH) {
    cutButtonPressed();
  }
  else if (coagButtonState == HIGH) {
    coagButtonPressed();
  }

  delay (50);                              // delay 50 ms to prevent bouncing
}

void LEDbuttonPressed() {
  if (LEDbuttonState == HIGH) {          // button went from off to on
    delay (50);                          // delay 50 ms to prevent bouncing
    //Debug
    Serial.println(LEDbuttonPushCounter);
    LEDbuttonPushCounter++;
    if (LEDbuttonPushCounter == 4) {   // counter at top of range
```

```
      LEDbuttonPushCounter = 0;        // reset counter to 0
   }
 }

 LEDlastButtonState = LEDbuttonState;   // save current state as last state for next loop

 switch (LEDbuttonPushCounter) {          // turns on LED module for incremented
brightness values
    case 1:
      analogWrite(illuminationLED, 64);     // brightness = low
      break;
    case 2:
      analogWrite(illuminationLED, 128);    // brightness = medium
      break;
    case 3:
      analogWrite(illuminationLED, 255);    // brightness = high;
      break;
    default:
      analogWrite(illuminationLED, 0);       // default = off if case does not match
      break;
 }

}

void suctionButtonPressed() {
 digitalWrite(suctionPump, HIGH);        // turn on suction pump
 delay(50);                              // time = 50 ms
 digitalWrite(suctionPump, LOW);         // turn off suction pump
 }

void irrigationButtonPressed() {
 digitalWrite(irrigationPump, HIGH);     // turn on irrigation pump
 delay(50);                              // time = 50 ms
 digitalWrite(irrigationPump, LOW);      // turn off irrigation pump
 }

void cutButtonPressed() {
 digitalWrite(cutLED, HIGH);             // turn on cut LED
 delay(50);                              // time = 50 ms
 digitalWrite(cutLED, LOW);              // turn off cut LED
 }

void coagButtonPressed() {
 digitalWrite(coagLED, HIGH);            // turn on coag LED
```

```
delay(50);                          // time = 50 ms
digitalWrite(coagLED, LOW);         // turn off coag LED
}
```

Brooke Barrow, B.S.
Elizabethtown, KY 42701
bebarr04@louisville.edu

EDUCATION

Master of Engineering in Bioengineering	04/18 (expected)
University of Louisville	GPA: 4.0 / 4.0
Louisville, KY	

Bachelor of Science in Bioengineering *with Honors*	05/2017
University of Louisville	GPA: 3.7 / 4.0
Louisville, KY	

WORK EXPERIENCE

Graduate Teaching Assistant	01/18 – 05/18
Department of Engineering Fundamentals	
Louisville, KY	

R&D Endomechanical Co-op	05/16 – 08/16
Ethicon-Endo Surgery, a Johnson & Johnson Company	
Cincinnati, OH	

R&D Energy Co-op	01/17 – 04/17
Ethicon-Endo Surgery, a Johnson & Johnson Company	
Cincinnati, OH	

R&D Mechanical Testing Lab Co-op	08/15 – 12/15
Ethicon-Endo Surgery, a Johnson & Johnson Company	
Cincinnati, OH	

Cardinal Ambassador	04/14 – 01/18
University of Louisville	
Louisville, KY	

LEADERSHIP EXPERIENCE

Student Body President	04/17 – 04/18
J.B. Speed School of Engineering	
Louisville, KY	

Sponsorship Coordinator	04/16 – 04/17
raiseRED Dance Marathon	
Louisville, KY	

Vice President of Operations	01/16 – 01/17
Kappa Delta Sorority – Alpha Xi Chapter	
Louisville, KY	

VOLUNTEER EXPERIENCE

Student Volunteer	12/17
International Service Learning Program (ISLP)	
Cebu City, Philippines	

HONORS & AWARDS

J.B. Speed School of Engineering Alumni Award	04/18

Henry Vogt Scholar	08/13 – 05/18
University of Louisville	

Research!Louisville, 1st place – M.Eng. category	09/17

Judi Olsen Endowed Scholarship	04/17
Department of Bioengineering	

Rho Lambda	01/16 – 05/17

Order of Omega	03/15 – 05/17

Honors Program	08/13 – 05/17
University of Louisville	

Patrick W. Halloran National Scholarship	12/15
Order of Omega	

Dean's List (x7)	12/13, 05/14, 07/14,
J.B. Speed School of Engineering	12/15, 07/15, 05/16,
	12/16

COMMITTEE ASSIGNMENTS & ADMINISTRATIVE SERVICES

Department Chair Review Committee   10/17 – 01/18
Department of Engineering Fundamentals

Administrative Plans & Policies Committee   08/17 – 04/18
J.B. Speed School of Engineering

Taskforce on Tuition and Fees Setting Committee   08/17 – 04/18
University of Louisville

Executive Board Committee Member   08/17 – 04/18
UofL Student Government Association

Diversity Committee Student Representative   08/16 – 04/18
J.B. Speed School of Engineering

External Advisory Board Student Representative   11/17
Department of Bioengineering

Diversity Week Planning Committee   08/17 – 10/17
J.B. Speed School of Engineering

ABSTRACTS & PRESENTATIONS

Speed Research Exposition, Louisville, KY   03/18
Barrow, B, Higginson C, Heidel, J, Pantalos, G, Roussel, T. Development of a Flight-Ready Multi-Functional Surgical Wand for Space-Based Surgical Applications.

Research! Louisville, Louisville, KY   09/17
Barrow, B, Higginson C, Heidel, J, Pantalos, G, Roussel, T. Development of a Flight-Ready Multi-Functional Surgical Wand for Space-Based Surgical Applications.